DAMAGE TOLERANCE OF TOUGHENED EPOXY AT LOW TEMPERATURES

By

Emel Manga

to obtain the degree of Master of Science

at Sabanci University,

to be defended on Wednesday, 27th July 2022 at 17:00.

Student Number: 27396

Thesis Committee:

Prof. Dr. Mehmet Ali Gülgün,	Sabanci University
Prof. Dr. Yusuf Ziya Menceloğlu,	Sabanci University
Prof. Dr.-Ing. habil. Bodo Fiedler	Hamburg University of Technology (TUHH)

Acknowledgement

This thesis marks the end of my Master's degree at Sabanci University, and I would like to express my deepest gratitude to the people who have touched my life to make everything so beautiful.

First of all, I would like to thank my beloved thesis supervisors Professor Melih Papila and Professor Mehmet Ali Gülgün from the bottom of my heart for always believing in me and seeing the potential in me throughout the three years. You taught me to be an independent and critical scientist by showing your enthusiasm for your work. I am very grateful to you for giving me the freedom I needed to find my interests during this time. Also, you were always willing to help me achieve my dreams and encourage me to push my limits whenever I needed to. Despite the many miles that separate us, it would not have been better without your support.

Furthermore, I would like to thank Professor Bodo Fiedler, Dr. Hans Wittich and MSc. Tobias Tiedemann for giving me the opportunity to do my master thesis on an exciting and novel topic at the Institute of Polymers and Composites. I really appreciate that they helped me and provided me with what I needed and more. Thank you for the fruitful weekly meetings and all the conversations we had both on a professional and personal level. I am very grateful to my colleagues at the Institute of Polymers and Composites for creating a nice work environment. Valea, Julian, Jonas, Katrin, and Melissa, I thank you for always helping me and for guiding me with your experience.

I would also like to thank my friends and colleagues at Sabanci University for all their help, discussions and friendship. Farzin, thank you for teaching me about composites, introducing me to the world of electrospinning and showing me your interest in electron microscopy. Thanks to you, the hours I spent in the labs became easier and you opened up the wonderful world of scanning electron microscopy to me. With your guidance, I certainly learnt a lot more. Shahrzad, I am so glad I met you. From the very beginning you showed me your patience, love and kindness. You always helped me a lot when I needed a breather. The time we spent together is so precious! To my friends Atike, Bilgen, Beril, Saba and Tuğçe: I have so enjoyed the time we have spent together, both in terms of our careers, our concerns, our goals and our personal growth. You have made this journey so beautiful and I will always be in touch with you. A big thank you to the Think Composites group, Dr Kaan Bilge, Dr Nursel Karakaya, Barış Emre, Berk Emre, Ecenaz, Melike, Rukiye, thank you for all the time we spent together and for teaching me so much during my time there. To everyone I may have forgotten to mention, thank you for being a part of my journey.

My deepest gratitude also goes to Ayşen Sarıoğlu Koşar and Koray Koşar. Since the first day I met you, you have always been my role models. Thank you from the bottom of my heart for always supporting me, lighting my way and always being a home for me.

To my family, I would like to express my undying gratitude for providing me with their love, care and support throughout the years. My wonderful mother and my beloved brother Emre, I am so lucky to have a family like you. Thank you so much for always believing in me, encouraging me

to go to other countries to better myself, and most of all for being a best friend to me. I do not want to know how I would be without you. I could not have succeeded without your support. I only appreciate for everything. Sizi her şeyden çok seviyorum! And, to my wonderful partner, Nasir, my special thanks to you for making everything amazing, accompanying me when I was working, for motivating me in hard and good times, for your unconditional love. You make my life every day brighter!

Emel Manga,

Hamburg, 2022

Table of Contents

Abstract

Epoxies are high performance thermosetting polymers widely used in many engineering applications such as structural adhesives, coatings and matrices of fiber reinforced polymer composites. They possess exceptional mechanical properties, chemical resistance, and high temperature properties. However, the highly cross-linked epoxy networks are inherently brittle, and therefore epoxy resins show a low resistance to crack propagation compared to other polymers. Meanwhile, numerous methods are used to improve their fracture resistance. For example, elastomers, core-shell particles or a second phase via domain precipitation are added to the epoxy to enable larger plastic deformation. Reinforcement with carbon nanoparticles has also been investigated.

New applications of epoxy resins and fibre-reinforced plastics can be found in the burgeoning hydrogen economy, which experiences a come-back to the World-stage as a promising protagonist especially with regards to the challenges of climate change to lower the CO_2 emission. Since the liquid hydrogen has to be kept in cryogenic conditions and pressurized, the hydrogen storage vessels should be designed based on cryogenic temperature conditions. The composites must be able to withstand very low temperatures and retain their functions even in face of sudden major temperature changes. In addition, they can lead to weight savings for applications where are subjected to uniform pressure that causes equal membrane strains. Like most materials, epoxy resin behaves much more brittle at low temperatures than at room temperature. Common tougheners are not designed for such temperatures and are sometimes based on mechanisms that no longer function when the material is “frozen”.

This present work investigates the mechanical properties, fracture performance and toughening mechanisms of a cured epoxy polymer modified by a second phase such as core-shell particles, elastomer particles or carbon-nanotubes (CNTs). To enhance fracture toughness of the epoxy resin, core-shell, elastomer and carbon nanotube (CNTs) tougheners were incorporated using different content ratios. Mechanical tests were carried out at different temperature conditions such as ambient, -40 °C and -80 °C. Different tougheners revealed different properties under different temperature conditions. The single edge notched bending (SENB) test results showed that fracture energy of the modified epoxy at -40 °C increased from 461 kJ/m^2 to 610 kJ/m^2 with the addition of 30 wt.% elastomer particles. When the temperature lowers, the largest increases in fracture energy observed were for 0.3 wt.% CNTs and 30 wt.% elastomer particles. The toughening mechanisms for such systems were postulated to be rubber-particle cavitation and void growth and debonding and plastic void growth of the silica necklaces.

Özet

Epoksiler, yapısal yapıştırıcılar, kaplamalar ve fiber takviyeli polimer kompozit matrisleri gibi birçok mühendislik uygulamasında yaygın olarak kullanılan yüksek performanslı ısıyla sertleşen polimerlerdir. Olağanüstü mekanik özelliklere, kimyasal dirence ve yüksek sıcaklık özelliklerine sahiptirler. Bununla birlikte, yüksek düzeyde çapraz bağlı epoksi ağları doğal olarak kırılgandır ve bu nedenle epoksi reçineleri, diğer polimerlere kıyasla çatlak yayılmasına karşı düşük bir direnç gösterir. Bu arada, kırılma dirençlerini geliştirmek için çok sayıda yöntem kullanılmaktadır. Örneğin, elastomerler, çekirdek-kabuk parçacıkları veya alan çökeltme yoluyla ikinci bir faz, daha büyük plastik deformasyonu sağlamak için epoksiye eklenir. Karbon nanoparçacıklarla güçlendirme de araştırılmıştır.

Epoksi reçinelerin ve elyaf takviyeli plastiklerin yeni uygulamaları, özellikle iklim değişikliğinin CO_2 emisyonunu düşürme zorluklarıyla ilgili olarak umut vaad eden ve günümüzde bu amaçlarla gelişen hidrojen ekonomisinde bulunabilir. Sıvı hidrojenin kriyojenik koşullarda tutulması ve basınçlandırılması gerektiğinden, hidrojen depolama kapları kriyojenik sıcaklık koşullarına göre tasarlanmalıdır. Kompozitler, çok düşük sıcaklıklara dayanabilmeli ve ani büyük sıcaklık değişimleri karşısında bile işlevlerini sürdürebilmelidir. Ayrıca, eşit membran gerilmelerine neden olan tek tip basınca maruz kalan uygulamalar için ağırlık tasarrufu sağlayabilirler. Çoğu malzeme gibi, epoksi reçine de düşük sıcaklıklarda oda sıcaklığından çok daha kırılgan davranır. Yaygın sertleştiriciler bu tür sıcaklıklar için tasarlanmamıştır ve bazen malzeme “donduğunda” artık çalışmayan mekanizmalara dayanır.

Bu tez çalışması, çekirdek-kabuk partikülleri, elastomer partikülleri veya karbon-nanotüpler (CNT'ler) gibi ikinci bir faz tarafından modifiye edilmiş kürlenmiş bir epoksi polimerin mekanik özelliklerini, kırılma performansını ve sertleşme mekanizmalarını araştırmaktadır. Epoksi reçinenin kırılma tokluğunu arttırmak için çekirdek-kabuk, elastomer ve karbon nanotüp (CNT'ler) sertleştiriciler farklı içerik oranları kullanılarak dahil edilmiştir. Mekanik testler oda sıcaklığı, - 40 °C ve -80 °C gibi farklı sıcaklık koşullarında gerçekleştirilmiştir. Farklı sertleştiriciler, farklı sıcaklık koşulları altında farklı özellikler ortaya çıkarmıştır. Tek kenar çentikli bükme (SENB) test sonuçları, -40 °C'de modifiye edilmiş epoksinin kırılma enerjisinin, ağırlıkça %30 elastomer parçacıklarının eklenmesiyle 461 kJ/m2'den 610 kJ/m2'ye yükseldiğini göstermiştir. Bu tür sistemler için sertleştirme mekanizmalarının, kauçuk-parçacık kavitasyonu ve boşluk büyümesi, bağların ayrılması ve plastik boşluk büyümesi olduğu varsayılmıştır.

List of Figures

List of Tables

1 Introduction

The introduction part of this thesis provides an overview of the reasons that made toughening mechanism of epoxy resin concepts worthy of investigating. In addition, it will illustrate the importance of fracture toughness tests at different temperature conditions. It follows by specifying the focus of this literature study, motivation and ends with the outline of the thesis structure.

This thesis is an investigation of an epoxy system that is modified to make it function properly at cryogenic temperatures. Each modified epoxy matrix was characterized for its morphology, thermal, tensile and fracture properties. Fractured samples were examined using scanning electron microscopy (SEM) techniques to explain the toughening mechanisms operating in each system.

1.1 Background

Due to its advantageous mechanical qualities, such as high specific strength and specific stiffness, carbon fiber reinforced composites are regarded as viable materials for use in the fuel tank structures of launch vehicles. However, in such vehicles, cryogenic liquids like liquefied oxygen and liquefied hydrogen are frequently utilized as fuel and an oxidizing agent due to high specific impulse considerations, respectively [2]. With such challenging fuels comes challenging conditions for their containers such as cycling between room temperature and cryogenic temperature as a load is applied. As if it is not enough, a composite tank used to store cryogenic liquids goes through cryogenic aging. Due to the different coefficients of thermal expansion between the fiber and matrix, as well as between different layers woven with different angles, microcracks may therefore develop in the composite matrix. Such structural damage causes the structures' mechanical characteristics to deteriorate, leading to phenomena such fiber/matrix interfacial debonding, potholing, and/or delamination, all of which are likely to cause liquid leakage [3,4].

The benefits and limitations of these materials as matrix for composites have been the subject of several studies since the invention of toughened polymer resins. When used in fiber reinforced composites [5,6], compositions [7,8], toughened epoxy resins with micro- or nano-sized stiff fillers such alumina and clay exhibit improved crack development resistance. Additionally, it has been shown that using clay and nanosized Al_2O_3 particles at cryogenic temperatures can increase delamination or crack resistance.

Epoxy resins are high class of thermosetting polymers which are widely used in many engineering applications as adhesives, coating, and matrices of fiber-reinforced composites. The right selection of epoxy resin and hardener, along with the ideal curing time enable such a broad range of industrial applications. The appealing properties of epoxy resins, such as high modulus, no creep, high strength and thermal and dimensional stabilities, have led to a rising interest in their usage in aerospace, automotive and marine industries [2]. However, due to highly crosslinked structure of epoxies which makes them brittle, they exhibit low toughness and poor impact resistance that leads

crack initiation and propagation for stress transfer applications [1,2]. Due to this brittle nature, the applied stresses will result in additional damage or propagate the existing cracks, which would significantly reduce the component's lifespan and could cause irreparable failure [9].

The importance of toughened matrices is even more emphasized as the World is facing a climate crisis making a reduction in the carbon footprint a necessity. Meanwhile, there is an increasing demand on alternative fuels, such as liquid hydrogen. Hydrogen economy may be one of the ways of mitigating the global emissions of greenhouse gases. To achieve this aim, specifically automotive and aerospace industries have focused on the use of liquid hydrogen as fuel, and therefore, on hydrogen storage vessels. The main requirement to store liquid hydrogen (LH2) is to keep it below -252 °C or 20.3 K which is the boiling point of dihydrogen at ambient pressure [10]. A liquid hydrogen vessel is made to retain a cryogenic liquid rather than to sustain internal pressure [11]. To minimize heat transfer, the vessel needs to be appropriately insulated [12]. As a result of heat transmission from the ambient to the liquid, the pressure inside the vessel rises. Due to the tank's inability to withstand high pressure, hydrogen is permitted to escape through a relief valve, a process also known as "boil-off" [13,14]. One of the main obstacles in using liquid hydrogen is to work with cryogenic temperatures which keeps liquid fuel below its boiling point., It is necessary to maintain hydrogen at cryogenic temperatures and to avoid boil-off. Material selection which withstands low temperature conditions plays a paramount importance. High strength, high fracture toughness, high stiffness, low density, and minimal H2 penetration are the ideal properties to have in a material for a tank wall [15]. In this regard, epoxy based composite materials are taken into consideration because of their low density and high strength.

In addition, a current research area is the suitable toughness adjustment of the epoxy materials to enable an optimal performance at low temperature conditions of liquid and gaseous hydrogen. To enhance the crack propagation resistance of epoxy resins at low temperatures, incorporating a second, tough/soft phase into the epoxy matrix to create a multi-phase composite is one of the most effective techniques to toughen epoxies [2–4]. Reactive liquid rubbers or thermoplastics are the traditional toughening agents used to introduce the second phase. Before the epoxy cures, these conventional toughening chemicals are dissolved in it, and when the epoxy cures, they phase separate to create distributed particles. This in-situ formation of a composite microstructure offers a new route to design tough composites. The new network can be made more flexible by lowering the crosslinking density and incorporating the high molecular weight second-phase additives that improve the resistance against cracking, specially at low temperature conditions [10].

The addition of rubber and rigid particles has shown to emphasize these properties without changing the thermo-mechanical properties of the epoxy resin [16].

Already at very low volume fractions, these latter toughеners effectively raise the critical stress intensity factor KIC (i.e., a measure of the direct increase in toughening behavior) and exhibit no filtration or viscosity changes as a result of the inherent precipitation that occurs during curing. In literature, the mechanisms of toughening at room temperature are well-known. However, low

temperature properties, particularly in fatigue crack propagation are not well addressed. However, such low-T properties are crucial for the creation of long-term cycled thermosetting composite parts, such as filament wound hydrogen vessels. Literature on composite hydrogen vessels also lacks detail in conjunction with applicable pertinent epoxy resin systems with a focus on industrial processing. In fact, low temperature performance of composite containers for fuel liquids, such as liquid hydrogen, where the storage tank experiences temperatures as low as 20 K, is a unique requirement for pressure vessels. Thus, research on materials with improved resistance to microcracking at cryogenic temperatures is emerging especially for applications involving thermoset polymers and fiber reinforcement [17].

In this thesis, core shell and elastomer particles as well as multi walled carbon nanotube (MWCNT) were studied as toughening agents for an epoxy resin system. Each combination of toughener group will be described in detail in the upcoming parts of the thesis.

1.2 Objectives and research areas

The main aim of this work was to investigate and identify the three particles to modify epoxy resin to enhance the fracture toughness at low temperature conditions. The core-shell, elastomer particles and multi walled carbon nanotube (MWCNT) modified the epoxy resin systems to provide higher fracture toughness (Kıc) and energy (Gıc) values at low temperature condition. The study aims to understand the appropriate toughening mechanism as well as to correlate the microstructures and the resulting properties of the modified epoxy resin systems.

1.3 Epoxy Resin

Epoxies are produced by polymerization (curing) reaction of epoxy resins in the presence of hardeners and/or catalysts. The final properties of the epoxy materials rely on the combination of the used epoxy and hardeners, the curing temperature, and the curing schedule. Therefore, it is crucial to understand the differences between the chemical and physical properties of unmodified epoxy materials and the modified epoxies.

The term “epoxy resins” refers to a class of monomers called oxirane/epoxy rings which are three-membered rings made up of an oxygen atom, two carbon atoms and one or two hydrogen atoms, respectively [18,19] as shown in Figure 1. Epoxy resins comprise more than these oxirane rings, which can be positioned internally or in cyclic structures and the number of oxirane rings per epoxy monomer determines the resin's functionality [20]. A suitable hardener, catalyst, or both can be used to activate the polymerization process. Epoxies are produced with a strongly cross-linked thermosetting structure after the polymerization reaction (curing) with hardeners/catalysts, and the epoxy rings serve as the cross-linking sites.

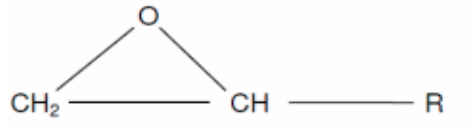

Figure 1: The epoxide end-group, R stands for the molecular structure of the remaining epoxy polymer [21].

One of the most widely used commercial epoxy resins is the diglycidyl ether of bisphenol-A (DGEBA) resin. As seen in Figure 2, it is created via the reaction of bisphenol A with epichlorohydrin in the presence of sodium hydroxide. Although DGEBA epoxy resin is a two-functional epoxy system, its molecular weight and viscosity can vary depending on the production conditions, the ratios of bisphenol A and epichlorohydrin, and other factors [2].

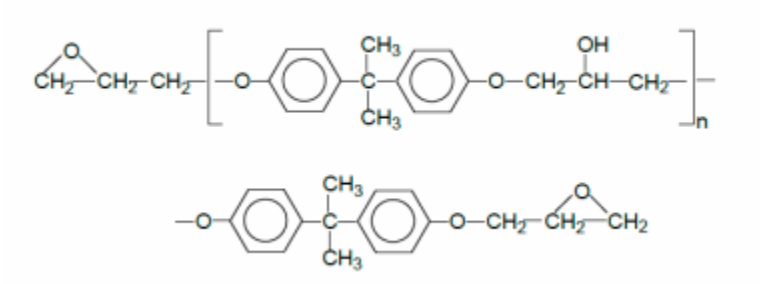

Figure 2: Molecular structure of DGEBA [22].

The repetition unit, n, in the middle of the DGEBA chemical chain, as shown in Figure 2, controls the variations in the molecular weights and viscosities of the DGEBA resin. The epoxy resin is a liquid with a viscosity in the range of 6,000 to 16,000 mPas when n is between 0.1 and 0.2; when n approaches 2, the resin solidifies [20,23].

Step growth polymerization and chain homo-polymerization are the two main polymerization (curing) processes of epoxy resins, and they are started by one or more curing agents and catalysts either individually or in combination [19,20]. Due to the fact that the curing reaction essentially uses a ring-opening mechanism, both polymerization reactions are exothermic, progressing without the generation of by products and with a low shrinkage rate.

Since the curing process of epoxy resin greatly affects the type of chemical bonds and the degree of cross-linking of the final epoxies, the choice of hardeners or catalysts mostly depends on the manufacturing needs and the final product requirements [20]. Additionally, one of the most crucial characteristics of cured epoxy resins is cross-link density, which is greatly impacted by the curing reaction. The tensile modulus, glass transition temperature, thermal stability, and chemical resistance are typically improved with increased cross-link density, while the flexibility and toughness of the epoxies are generally reduced [18,20].

Since epoxies are brittle, their failure occurs most frequently in fracture in a tensile stress field, where the issues of stress concentrations at defects (cracks) become significant. Since these

epoxies are extremely brittle materials with only localized plastic deformation during fracture, the fracture behavior of these materials has mostly been explored through the application of linear elastic fracture mechanics (LEFM) [24]. Therefore, the critical strain-energy release rate, Gc, (also known as the fracture energy), or the critical stress intensity factor, Kc, under plane strain circumstances are typically used to quantify the resistance to fracture for epoxies.

Unmodified epoxies typically have a Mode I fracture energy, or GIc, in the range of 100–300 J/m2 at room temperature. This falls into the category of extremely brittle materials and is almost never higher than thermoplastics with a comparable Tg. Although the values of GIc are far larger than the energy theoretically expected for purely brittle fracture, energy dissipation activities in the form of plastic deformation must nevertheless occur during fracture [24,25].

1.4 Toughening of Unmodified Epoxy Resins

1.4.1 Toughening by Core-Shell Particles

Using core-shell particles is an alternate method to enhance the toughness of epoxy polymers. These particles have a tougher shell surrounding a soft rubbery core. Typically, emulsion polymerization creates the particles, which are subsequently disseminated in epoxy resin. As a result, unlike phase-separating rubbers, it is simple to manufacture particles with controllable particle size. Multilayer particles are typical, and a variety of core and shell materials are possible [26]. In order for the shell to work with the epoxy polymer, poly (methylmethacrylate), which is occasionally functionalized, is frequently utilized. Polybutadiene [27] and acrylate-polyurethane rubbers [28] are examples of common core materials. According to the references [29–32], they have been proven to improve the toughness of both bulk polymers and fiber composites. In addition to discussing some of the additional qualities that can be impacted by the introduction of core-shell particles, Hayes and Seferis [33] have evaluated the use of core-shell particles in thermoset polymers and composites. When compared to liquid rubbers, these particles offer improved thermo-mechanical properties. Additionally, it is possible to effectively manage the particle size and volume percentage.

The static and fatigue fracture behavior of DGEBA epoxy hardened by core-shell particles was studied by Becu et al. [30]. They discovered that adding core-shell particles up to 24 vol. percent caused epoxy polymers' fracture toughness and impact strength to continuously rise. Similar to that, the inclusion of the modifier content was reported to reduce the rate of fatigue crack propagation.

The fracture energy of an epoxy resin tailored by the inclusion of core-shell particles increased from 77 J/m2 for unmodified epoxy to 860 J/m2 with 15 wt.% of 100 nm diameter core-shell particles particles, which was roughly an 11-fold increase, by Giannakopoulos and Masania [34]. Chen and Kinloch [22] added pre-formed polysiloxane core-shell particles with a mean diameter of 0.18 mm to an epoxy resin that had been hardened using an anhydride hardener. They

investigated the fracture energies of the epoxy polymers treated with core-shell particles throughout a temperature range of 20 °C to -109 °C. They observed that at both ambient temperature and cryogenic temperatures, core-shell particles considerably increased the fracture toughness.

1.4.2 Toughening by Elastomer Particles

The way the rubber particles are introduced allows us to divide this technology into two categories. The first method relies on the use of reactive liquid elastomers like butadiene-acrylonitrile (CTBN) rubber. These liquid reactive elastomers are typically made as an adduct (i.e., by first pre-reacting the rubber with epoxy) and combined with the epoxy resin. During the epoxy's curing process, the rubber particles are created on the spot. Because the in-situ production of the rubber particles is determined by the degree of compatibility between the reactive liquid elastomer and the epoxy precursor, as well as by the kinetics of gelation, this strategy does not give good size and volume fraction control of the rubber particles [1].

The final pre-polymer of CTBN modified epoxy resin is typically diluted with more ER before curing. The microstructure created is made up of an elastomeric phase that is finely dispersed in the epoxy matrix, and the final material's impact behavior is significantly influenced by the size of the produced elastomeric particles [35].

Diglycidyl ether of bisphenol A (DGEBA) epoxy was modified by McGarry et al. using a liquid CTBN copolymer and curing with 2,4,6-tri(dimethylaminoethyl) phenol (DMP) (McGarry 1970; Sultan et al. 1971; Sultan and McGarry 1973). The results demonstrated that, at the ideal rubber concentration (about 7.5 wt.&), the fracture toughness of modified epoxy resin by an order of magnitude (McGarry 1970 [36].

The effect of temperature on the fracture toughness of a CTBN modified epoxy was investigated by Bascom and Cottington [37]. It was found that GIc enhances non-linearly in an accelerated way with temperature over the range of -40 to 50 °C (233-323 K), see Figure 3.

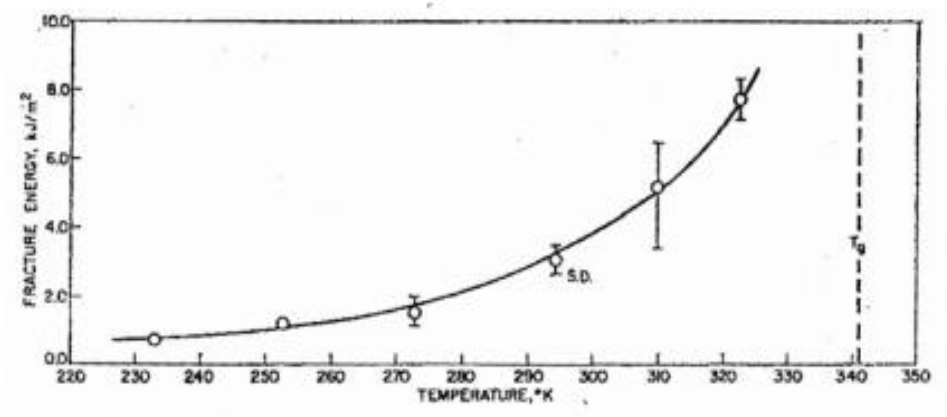

Figure 3: Bulk fracture energy, Gıc, versus temperature for a 15 wt.% CTBN modified epoxy [38].

Using a quantitative model, Huang and Kinloch [39] investigated the contribution to toughness increase from localized shear band yielding, void formation, and rubber bridging in a CTBN rubber modified epoxy. At room temperature, the localized shear band yielding and plastic void expansion account for 54 % and 38 %, respectively, of the total energy released during fracture, whereas rubber bridging only contributed 8 %. These findings support the significant roles of localized shear band yielding, plastic void expansion, and rubber bridging in rubber particle modified epoxies.

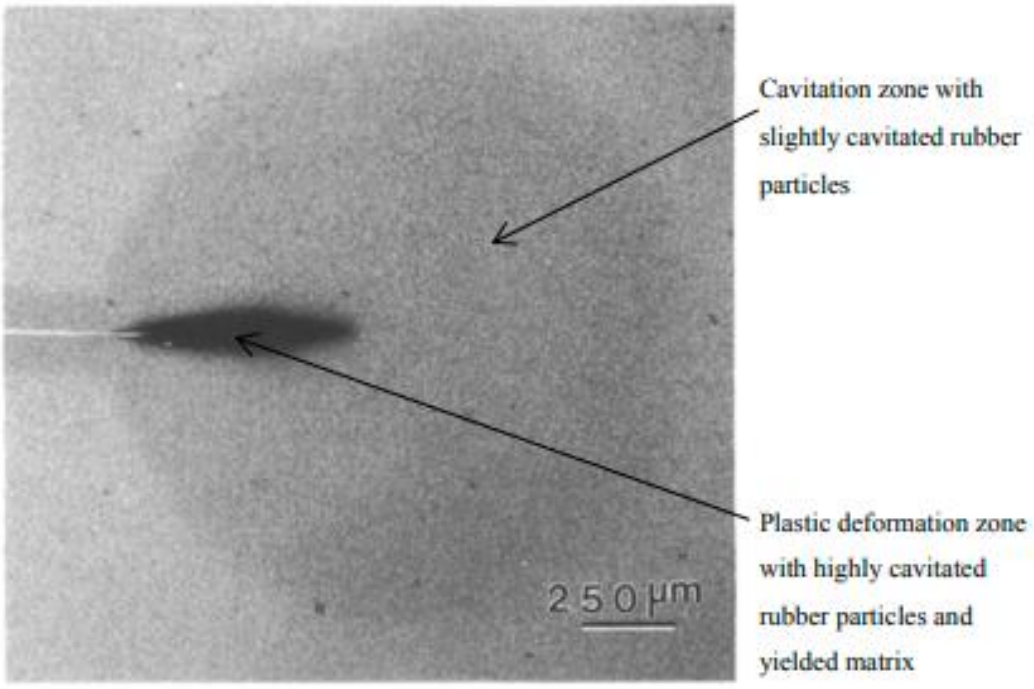

Figure 4: Transmission optical micrograph image of the initially loaded crack tip of a CTBN modified epoxy [32].

1.4.3 Toughening by Multi Walled Carbon Nanotubes (MWCNT)

Rolling graphene sheets with hexagonal carbon rings into hollow cylinders creates carbon nanotubes. A single-walled carbon nanotubes (SWNT) comprises a single graphene cylinder with a diameter of between 0.4 and 3 nm and a fullerene hemisphere cap Nanotubes vary in size from a few hundred micrometers to millimeters. The nanotubes display exceptionally large aspect ratios as a result of their properties. SWNTs can typically assemble into ropes because to the strong van der Waals attractions that exist between their surfaces. A 0.34 nm interlayer gap distinguishes the 2 to 50 coaxial cylinders that comprise multi-walled carbon nanotubes (MWNT). MWNTs typically have a diameter between 4 and 30 nm [40]. The structure of the concentric graphene cylinders in MWNTs is reminiscent of a Russian doll. A nanofiber, on the other hand, is made up of layered, curved graphite layers that resemble cones or cups [41].

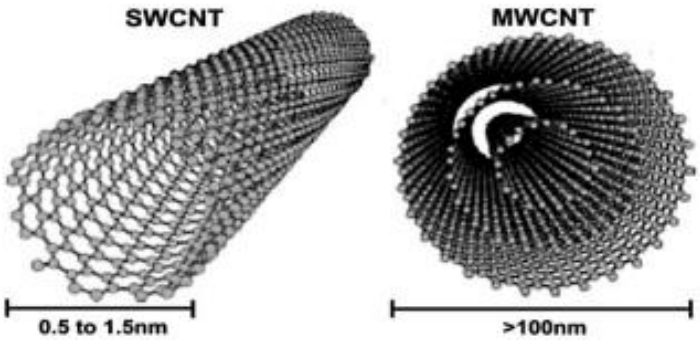

Figure 5: Illustration of single walled carbon nanotube (left) and multi walled carbon nanotube (right) [42].

Besides its definition, carbon nanotubes (CNTs) are a promising reinforcing material for polymer matrix composites because to their remarkable mechanical properties, high aspect ratio, and large specific surface area [43,44]. CNTs can be used as an alternative reinforcing filler to improve mechanical characteristics as well as crack growth resistance, according to certain earlier studies [45,46]. They can act as bridges between crack surfaces and cause mechanical interlocking with the matrix material. A CNT-modified matrix and conventional fiber reinforcements have recently been demonstrated to increase matrix-dominated parameters including interlaminar shear strength [47].

Carbon nanotubes (CNTs) have desirable candidates for use as toughening agents in epoxy resins and fiber-reinforced epoxy composites due to their exceptional mechanical properties. According to Tang et al. [48], adding 1 wt.% MWCNTs to an epoxy raised the mode-I fracture energy by 56 % while simultaneously increasing the Young's modulus. According to Cha et al. [49], adding 1 wt.% of poly(4-aminostyrene) functionalized CNTs to an epoxy resulted in an increase in the tensile strength and Young's modulus from 2.76 GPa to 3.89 GPa, respectively. In a different work, carbon nanotubes that had been non-covalently functionalized were used by Cha et al. [37] to improve the epoxy nanocomposites. Young's modulus, ultimate tensile strength, and fracture toughness all showed considerable improvements, with 64 %, 22 %, and 95-100 %, respectively. Mode-I, mode-III, and mixed-mode fracture toughness of MWCNT/epoxy nanocomposites were measured by Saboori et al. [50]. As the MWCNT concentration grew to 0.5 wt%, it was observed that the mode-I fracture energy continuously increased by 27 wt%, and then marginally dropped for 1 wt% MWCNTs. Mode-III and mix-mode fracture toughness saw more noticeable improvements, and as the MWCNT concentration rose to 1 wt.%, there was no downward trend. It is interesting that enhancing the mechanical and fracture properties of CNT modified epoxies by adding third phase modifiers, such as nanoclay [51], shows promise. Generally speaking, the mode-I fracture toughness might be considerably increased by the inclusion of a tiny number of MWCNTs. However, little research [52] has been done to examine the impact of CNTs on the behavior of epoxies during mode-II fracture, and the fracture mechanisms are still not fully understood.

Fiber reinforced epoxy composites (FRPs) typically contain CNTs that are either grafted or grown directly onto the carbon fibers [53] or added as CNT/fibre interleaves between the laminates [54]. Continuous carbon nanotube film was used by Xu et al. [53] as an interleave to improve CFRPs. With the addition of 0.22 wt.% CNT film, the flexural strength and interlaminar shear strength were enhanced by 16 and 25 %, respectively. To increase the interlaminar fracture toughness of CFRPs, Zheng et al. [54] created sandwiched carbon nanotube/polysulfone nanofiber (CNTs/PSF) papers as interleaves. According to one study, adding 10 % CNT/PSF interleaves to CFRPs increased the fracture toughness in the mode-I and mode-II directions by 53 % and 34 %, respectively.

Additionally, improvements of 27 % and 29 % in flexural strength and modulus, respectively, were made. The impact of using interleaves made of hierarchical carbon nanotube-short carbon fiber (CNT-SCF) on the interlaminar fracture toughness of CFRPs was examined by Zhou et al. [55]. The addition of 1.0 and 2.0 mg/cm^2 CNT-SCF interleaves increased the fracture toughness by 125 % and 98 % when compared to the control material. Fluorine functionalized CNTs were successfully deposited on the mid-plane of fiber reinforced epoxy composites by Davis and Whelan [56]. The energy of the mode-II fracture propagation rose from 1906 J/m^2 under control to 2419 J/m2 after the addition of 0.5 wt.% CNTs.

CNTs were generated in-situ on carbon fibers employing a flame synthesis technique in another study [57]. After only 3 minutes of CNT growth, the interfacial shear strength of the CFRPs was raised by almost 70 %. It is evident from the literature review that adding a little quantity of CNTs to the mid-plane of FRPs could greatly improve fracture toughness. However, only a small amount of research has used CNT modified epoxies as CFRP matrix to examine the fracture behavior of such composite laminates. Studies on the mode-I and mode-II fracture mechanisms of CFRPs based on CNT modified epoxy are also lacking.

1.5 Research Question and Motivation

This thesis focuses on the modified epoxy resins with different filler content rations for deeper understanding of which additive will work better into the epoxy systems. Moreover, the modified epoxy will be mechanically tested at different temperature environments to investigate the fracture toughness of the new epoxy systems at lower temperatures. Combining the gaps from the above-mentioned literature, the main thesis questions are shaped as:

1.) Which toughener can perform better to enhance fracture toughness of the modified epoxy?

2) Which content ratios can be considered optimal amounts of tougheners for better modified epoxy with ideal mechanical properties at low temperatures?

2 Materials and Experimental Procedure

The objective of this chapter is to give information about the materials used, and to describe the experimental methods that were followed to obtain the material properties and the various microscopic images. This chapter is divided into five sections. The first section gives information about the toughening agents and the epoxy systems employed. The second section explains the manufacturing processes for the unmodified/modified bulk epoxies and the fiber reinforced composites. The third and the fourth sections detail the mechanical tests that were used to characterize the properties of the bulk epoxies and the fiber reinforced composites respectively. The last section is devoted to a summary of the microscopy techniques that were used.

This chapter elaborates on all the materials, manufacturing methods and characterization techniques used to carry out this research during the thesis.

2.1 Materials

2.1.1 Epoxy Resin and Curing Agents

In this work, Epikote 828 manufactured by Hexion (United States) was used as the epoxy resin material to produce the unmodified and modified bulk-polymers. The epoxy resin comprises of bisphenol A-diglycidyl-ether (DGEBA). Epikote 828 has high mechanical and chemical resistance properties when the epoxy polymer is cured with various curing agents [58]. The chemical structure of epoxy resin was depicted in Figure 6

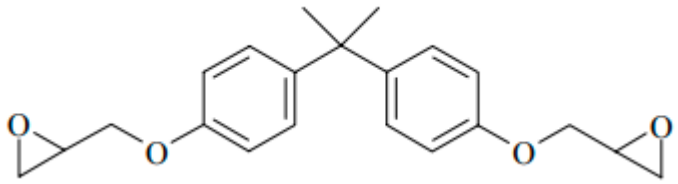

Figure 6: Bisphenol A-Diglycidylether (BADGE or DGEBA) [59].

Table 1: Properties of Epikote 828 [58].

Density in kg/L	1.16
Epoxy Group Content in mmol/kg	5260 - 5420
Viscosity at 25 °C in Pas	12-14
Epoxy Molar Mass in g/equivalent*	184 - 190
Remarks	Standard unmodified bisphenol A resin

As the curing agent, Epikure RIMH 137 from Momentive (United States) was used. RIMH137 [60] consists of poly(oxypropylene) diamine (50 -75 wt.%) and 3- aminomethyl-3,5,5-trimethylcyclohexylamine (35 -50 wt.%) [61].

Table 2: Properties of RIMH 137 [61].

Density in g/cm^3	0,93 - 0,98
Viscosity in mPas	10 - 50
Mixing Ratio Resin Epikote 828: RIMH137	100:28 ± 2
Amine Equivalent	52 eq/g

According to the manufacturer specification, the mixing ratio to be cured is 100:28 ±2 (Table 2) epoxy resin to curing agent by weight to meet a stoichiometric composition.

2.1.1.1 Determination of Viscosity

The rheological properties of epoxy resin as it cross-linked were carried out in rheometer ARES RDA-III 28 (TA Instruments) apparatus. The tests were executed on blended samples of Epikote 828 and RIMH 137 considering the mixing ratio between the materials**.** The machine was set up with 40 mm diameter of aluminum parallel plates at a gap distance of 500 µm. The viscosity was measured at 10 Hz constant rotational frequency and 10 % strain and for time-sweeps (isothermal) and temperature-sweeps (non-isothermal) test conditions.

A temperature range 25 °C (room temperature) to 80 °C with the 0.5 °C/min ramp rate for the non-isothermal tests and at 50 °C at constant temperature during 4 hours for the isothermal test.

2.1.2 Carbon-Nanotubes and Dispersion process of Carbon Nanotubes through Three Roll Milling

A NC7000 cylindrical multi walled carbon nanotubes in powder form, provided by Nanocyl (Belgium), with the decomposition temperature of 565 °C was used as the toughener in an epoxy polymer composition. In order to incorporate the carbon-based nanoparticles into the epoxy resin, three roll milling method was used for dispersion purposes. As shown in Figure 7, the working principle of three roll milling which comprises of three calendars is to rotate those cylinders in opposite directions by decreasing the gap sizes as well as increasing angular velocities simultaneously. It is also worth to mention that those gap sizes can be adjustable. In this thesis, the gap sizes and steps were adjusted by applying the shear forces as seen in Table 3.

Table 3: Three roll milling process parameters.

Step	Gap-1 in µm	Gap-2 in µm
1	120	40
2	40	13
5	13	5

The mixture of epoxy resin and carbon nanotube particles were placed into the feeding gap and dragged into the calendars.

Strong particle interactions are produced by large specific surface areas that are produced by high aspect ratios [62]. Separating the particles and adjusting their distribution is difficult [63].

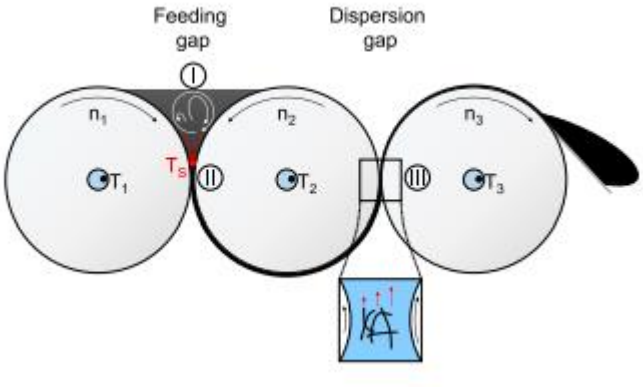

Figure 7: Schematic of Three Roll Milling Process of Carbon Nano Particles [61].

2.1.2.1 Rheological Studies of Carbon Nanotube and why we have chosen 0.3 wt.%?

As can be seen in Figure 8 which was conducted at isothermal test condition, between 0-6000 seconds of the test, it was found that the viscosity value of the 0.3 wt.% MWCNT. In the beginning of the rheology test, the viscosity showed that each MWCNT has different values because of the different content ratios. For 0.5 wt.% NC 7000, since it has the highest carbon nanotube amount in it, the viscosity values were higher than 0.3 wt% and 0.1 % NC 7000. With the time, the viscosity reached the certain point, which is saturation, for each group. That is the reason of why the viscosity values remains constant at the end of the experiment. Moreover, viscosity is a crucial parameter for composite processing since when a manufacturer has a low viscosity matrix, it cannot stick to fibers during the processing. Additionally, when a manufacturer has a matrix which has high viscosity, this time rollers cannot turn because of the dense matrix materials.

Besides this, it was found that for the composites which contains MWCNT modified epoxy matrix met the results which was investigated by Voorman [61]. According to previous results, the optimum viscosity value of a modified epoxy should be between 2-8 Pas since those results are sufficient for making composite materials at our facilities.

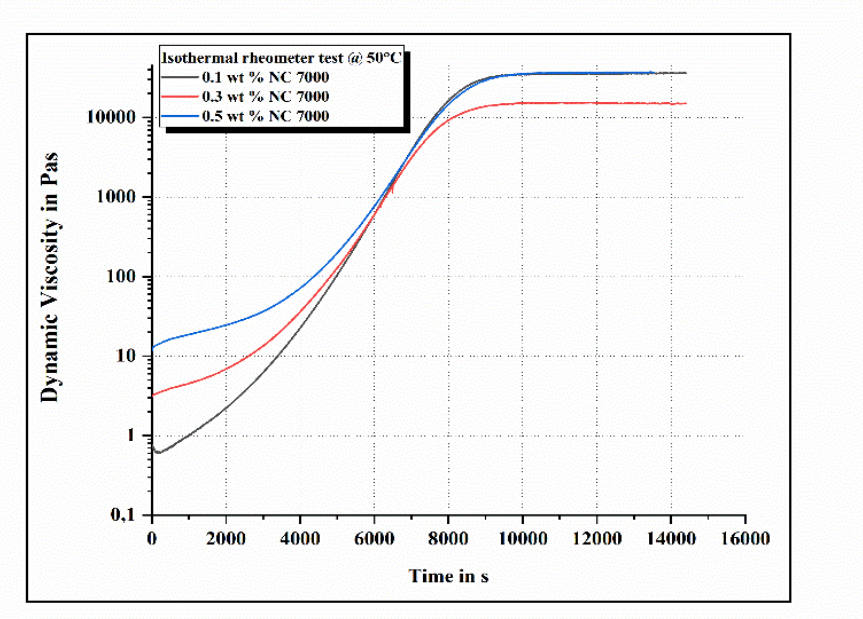

Figure 8: Rheology results of MWCNT at isothermal condition.

On the other hand, the same amounts of the MWCNT were tested at the non-isothermal environment. The temperature range was chosen from the ambient temperature to 80 °C for providing the curing temperature conditions of the epoxy resin. Based on Figure 9 it was observed that the rheology of the 0.3 wt.% MWCNT modified epoxy was between the above-mentioned ranges. For this thesis study, because of these reasons, 0.3 wt.% was chosen to modify the epoxy resin for enhancing the fracture toughness.

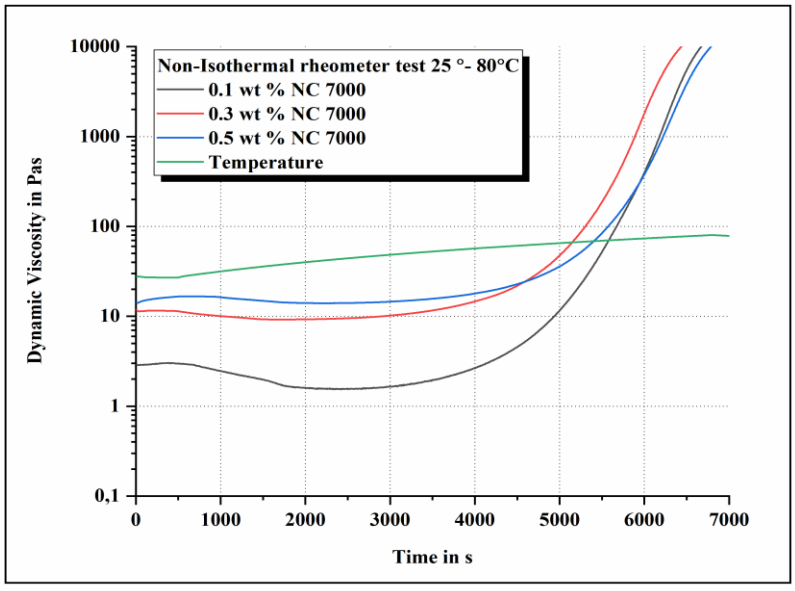

Figure 9: Rheology results of MWCNT at non-isothermal condition.

2.1.3 Core-shell particles

In the present study, Struktol Polycavit 3565, supplied by Schill + Seilacher (Germany), core-shell particles were used as the toughener in order to improve the fracture toughness of the epoxy resin. The core-shell particles comprise of soft core and glassy shell as depicted in the Figure 10. These core-shell/polyetheramine particles were designed to have a diameter of 40 nm, provided as a masterbatch of particles pre-dispersed at 40 % in a DGEBA epoxy resin with an epoxy equivalent weight (EEW) of 325 g/eq [64].

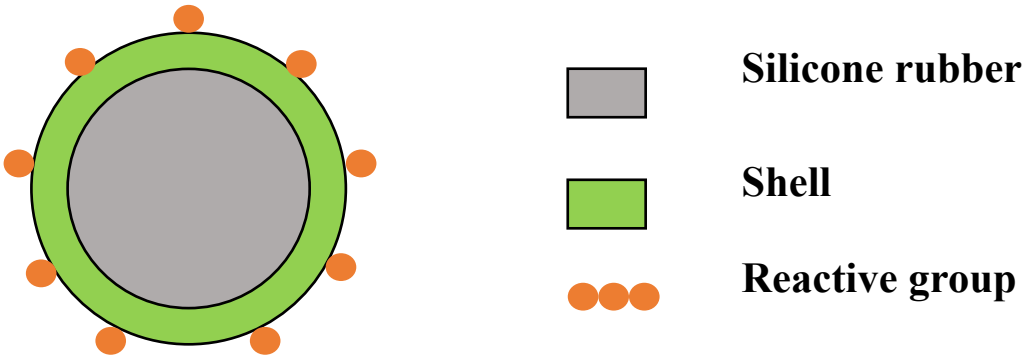

Figure 10: Schematic representation of core-shell particles. Adapted from [1].

2.1.3.1 Rheological Studies of Core-Shell Particles

To understand the viscosity behavior with the different test environments, rheology tests were carried out for core-shell particles for 10 wt.% and 20 wt.% filler contents.

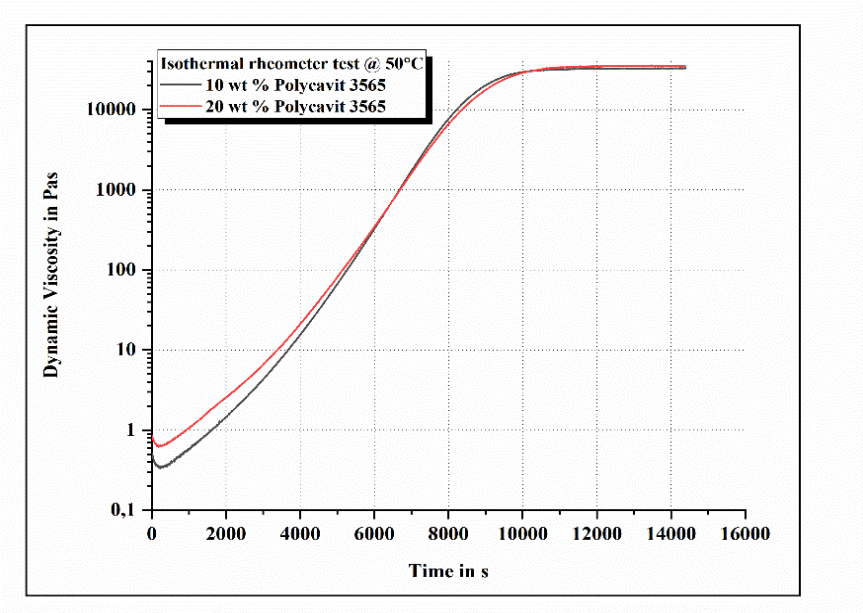

Figure 11: Rheology result of core-shell particles at iso-thermal condition.

As mentioned in previous section, the rheology tests were carried out under two different environmental conditions which are isothermal and non-isothermal. For further investigations the two modified epoxy, i.e., with 10 wt.% and 20 wt.% filler contents were chosen to compare minimum and maximum amounts on fracture toughness.

Figure 11 and Figure 12 give the rheological behavior for the core-shell modification at isothermal and non-isothermal test conditions, respectively. In Figure 12, in non-isothermal test set-up, 20 wt.% elastomer modified epoxy exhibited the higher viscosity behavior since it has a higher filler content in comparison to 10 wt.% elastomer modified epoxy.

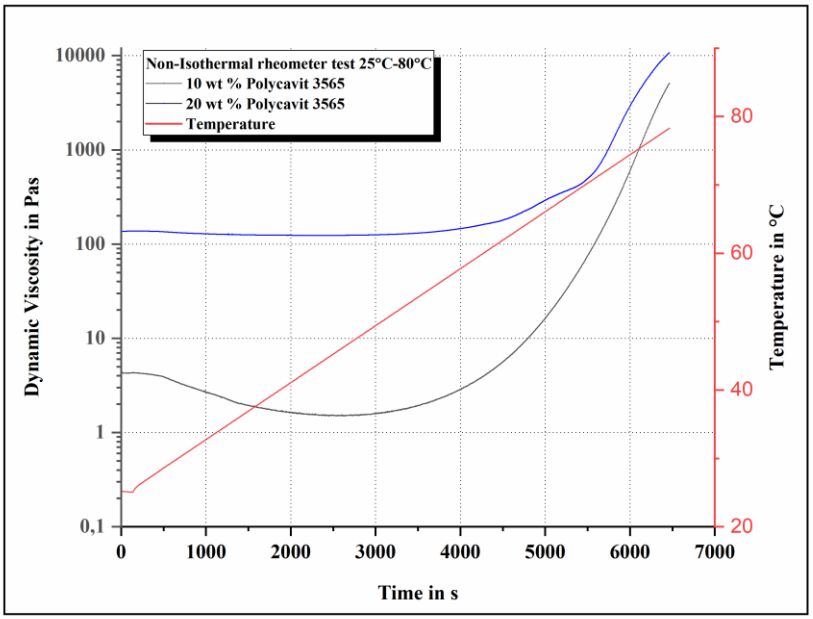

Figure 12: Rheology result of core-shell particles at non-isothermal condition.

2.1.4 Elastomer Modifiers

A Struktol Polydis 3614 carboxyl-terminated butadiene-acrylonitrile (CTBN) from Schill+Seilacher (Germany) was used as the elastomer particle. These rubber particles were designed to have the viscosity of 470 Pas at 25 °C, produced as a masterbatch of particles at 10-35 % in a DGEBA epoxy resin with an epoxy equivalent weight (EEW) of 330 g/eq [65].

2.1.4.1 Rheology of Elastomer Modifiers

For the same purposes, to understand the viscosity behavior of modified epoxy with the elastomer additives under the specific temperature conditions, isothermally and non-isothermally rheology tests were conducted. In Figure 13 it shows the isothermal test results for 20 wt.% and 30 wt.%. these filler content amounts were chosen to compare lower and higher filler amounts on fracture

toughness. It is also worth to point out that 20 wt.% elastomer and 20 wt.% core-shell additives can be compared in terms of the same amount but different type of modifiers.

In isothermal test results, since the viscosity ratio was between 2-8 Pas that has been explained in the previous section, these values were chosen for manufacturing purposes.

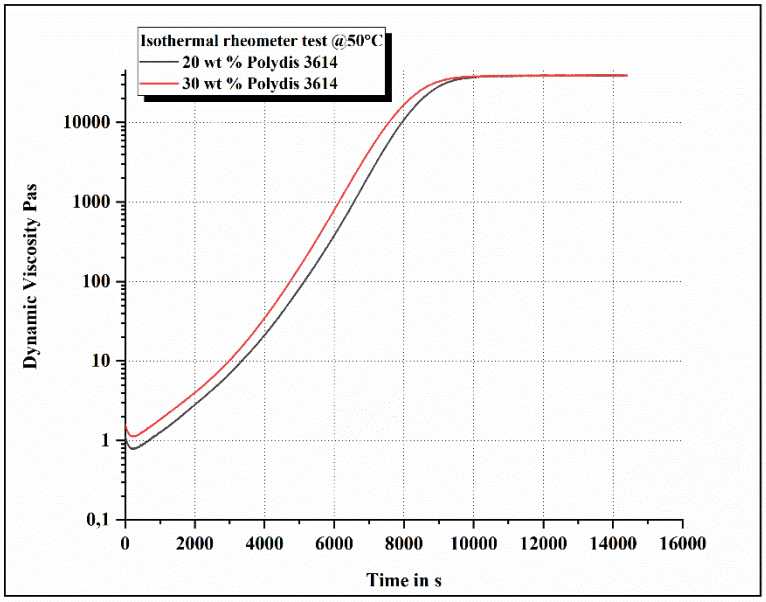

Figure 13: Rheology result of elastomer additives at isothermal condition.

In Figure 14, viscosity results at non-isothermal conditions, from room temperature to 80 °C, were obtained. For 20 wt.% and 30 wt.%, the viscosity values in the beginning of the test were between 2-8 Pas. Also, the blue line shows the temperature changes.

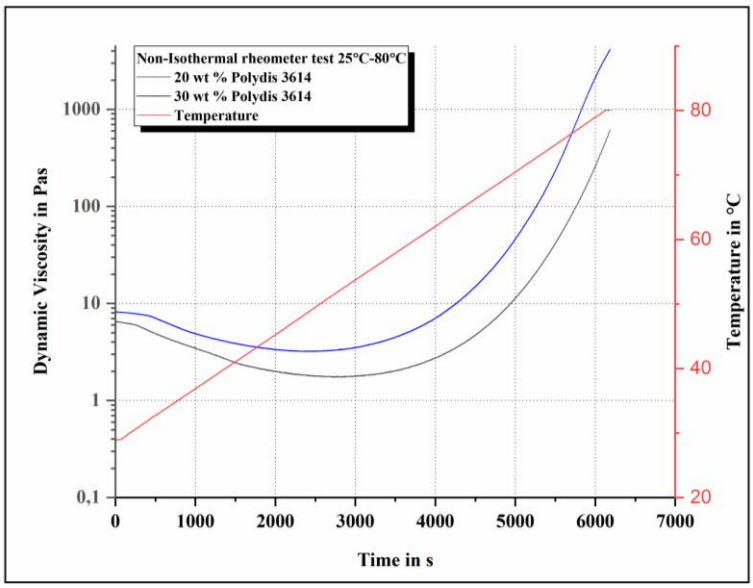

Figure 14: Rheology result of elastomer additives at non-isothermal condition.

2.2 Manufacturing of bulk epoxy samples - Manufacturing-degassing, curing parameters.

This section outlines the methods employed to manufacture the bulk samples.

The bulk specimens were prepared considering the mixing ratios between the constituents as shown in Table 4. Initially, the molds for casting were cleaned with isopropanol and coated with release agent (MİKON) followed by 10 minutes to dry. Afterwards the molds were assembled and preheated in the oven at 50 °C for the preparation of curing.

Meanwhile, polymer blending was prepared by mixing the epoxy resin and the hardener with the relevant amounts of tougheners by using a mechanical stirrer for degassing purposes for 10 minutes at 1 atm. After this proses, the mixture was poured into the Aluminum mold to produce the bulk unmodified and modified plates. Curing temperature for the oven (Memmert, Germany) was set at 50 °C for 4 hours and the post-curing at 80 °C for 12 hours with 5 °C/ min ramp rate.

Table 4: Content ratios of additive in bulk epoxy resins.

Group	Resin Hardener Ratio	Toughener Weight
Neat	100:28	-
MWCNT	100:28	Desired total mass*0.3%
Elastomer 20 wt.%	100:24	Resin*20%*0.01
Elastomer 30 wt.%	100:23	Resin*30%*0.01
Core-Shell 10 wt.%	100:27	Resin*10%*0.01
Core-Shell 20 wt.%	100:26	Resin*20%*0.01

The produced plates were cut initially using the mechanical cutter saw blade (QATM, Germany) with 0.400 mm/s speed and inserted the notches using the razor blades for the preparation of mechanical test specimens like in Figure 15. The crack length will be also explained in Table 4.

2.3 Thermal and mechanical tests for bulk polymers

2.3.1 Dynamic Mechanical Thermal Analysis (DMTA)

In order to determine the glass transition temperature of the bulk epoxy samples, dynamic mechanical thermal analysis (DMTA) was carried out in a Gabo Eplexor 500 N (NETZSCH GABO Instruments) DMTA between -150 °C and +150 °C with the heating rate of 2 K/min in tensile mode by applying cyclic loads. The test parameters were set to clamping distance 30 mm and test frequency at 1 Hz. The test result will be discussed in detail in Section 3.

2.3.2 Single-Edge Notch Bend (SENB) Tests

The aim of this experimental test part was to obtain information on the Kıc and Gıc sensitivity of particle modified epoxies at different temperature conditions for the described aspects.

In accordance with the ASTM D-5045-99 standard, the single-edge notch bending tests were executed in a Zwick/Roell Z2.5 universal testing machine on the unmodified and particle modified epoxy specimens in order to examine the fracture toughness values [66]. Mechanical tests were carried out at room temperature, -40 °C and -80 °C for each specimen groups. The test conditions will be detailed in the upcoming sections.

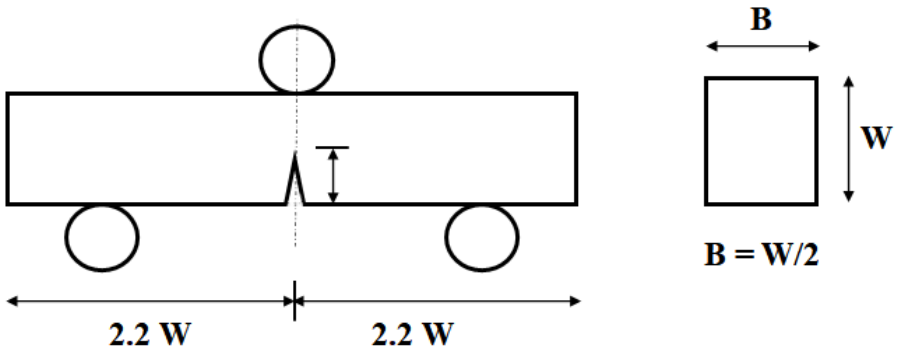

Figure 15: Single-Edge Notched Bending Test Specimen Configuration [66].

The size and the geometry of the specimens were prepared with respect to the ASTM D-5045-99 prescription as shown in the Figure 15. Based on the configuration, all specimen thicknesses, width, and pre-crack lengths are shown in the Table 5. All dimensions confirm the test specifications.

Table 5: Specimen dimensions for SENB test.

Specimen	Thickness (cm) (B)	Width (cm) (W)	Crack Length (cm) (a)
Neat Epoxy	0.39	0.78	0.35
10 wt.% core-shell	0.39	0.78	0.39
20 wt.% core-shell	0.39	0.77	0.35
20 wt.% Elastomer	0.40	0.77	0.36
30 wt.% Elastomer	0.39	0.79	0.40
0.3 wt.% MWCNT	0.39	0.76	0.39

Mode I fracture toughness, K_{1c}, values of the tested specimens were calculated using the formula below:

$$K_{1c} = \left(\frac{P}{BW^{1/2}}\right) f(x) \tag{2.1}$$

where ($0.2 < x < 0.8$):

$$f(x) = 6x^{1/2}\,\frac{[1.99 - x(1-x)(2.15 - 3.93x + 2.7x^2)]}{(1+2x)(1-x)^{3/2}} \tag{2.2}$$

$$x = a/W \tag{2.3}$$

where P is the maximum load, B is the specimen thickness, W is the specimen width and a is the crack length.

2.3.2.1 Room Temperature (25 °C)

All specimen groups which comprise of neat, core-shell particles, elastomer and MWCNT modified epoxies were tested at room temperature condition based on the test standard. All parameters were set and SENB mechanical tests were executed.

2.3.2.2 Measurements at -40 °C

To lower the temperature from ambient to -40 °C, the cooling chamber was set -40 °C using the machine Weisstechnikk (Germany) as seen in Figure 16. In this figure, cooling machine helps to cool down the test environment for -40 °C. It comprises of two hoses which are lower and upper. Upper hose is responsible for cooling the environment and this air circulates inside of the metallic box. Afterwards, circulated air is absorbed from the lower hose. Therefore, the necessary temperature conditions are set.

Figure 16: Test set up for -40 °C. a) Cooling machine which has two hoses, upper and lower. b) Upper and lower hoses are connected to the test chamber. c) SENB test configuration with the specimen.

2.3.2.3 Measurements under Liquid Nitrogen

In this test condition, the liquid nitrogen was used to lower the ambient temperature to -80 °C by taking the advantage of boiling point of liquid nitrogen which is -195.8 °C as well as the precooling of the test setup. To do this, all specimen groups were cooled down inside of the liquid nitrogen filled Dewar bucket before conducting the mechanical testing. On the other hand, the steel and the plastic bucket part (see in the Figure 17) were pre-cooled in the cooling chamber, Weisstechnik (Germany), at -80 °C.

The upper part of the in-house built bucket was manufactured using high density polyethylene (HDPE) since this material has good insulation properties and a resistance to liquid nitrogen atmosphere while the lower part of the bucket was made of glass fiber reinforced epoxy (GFR/epoxy).

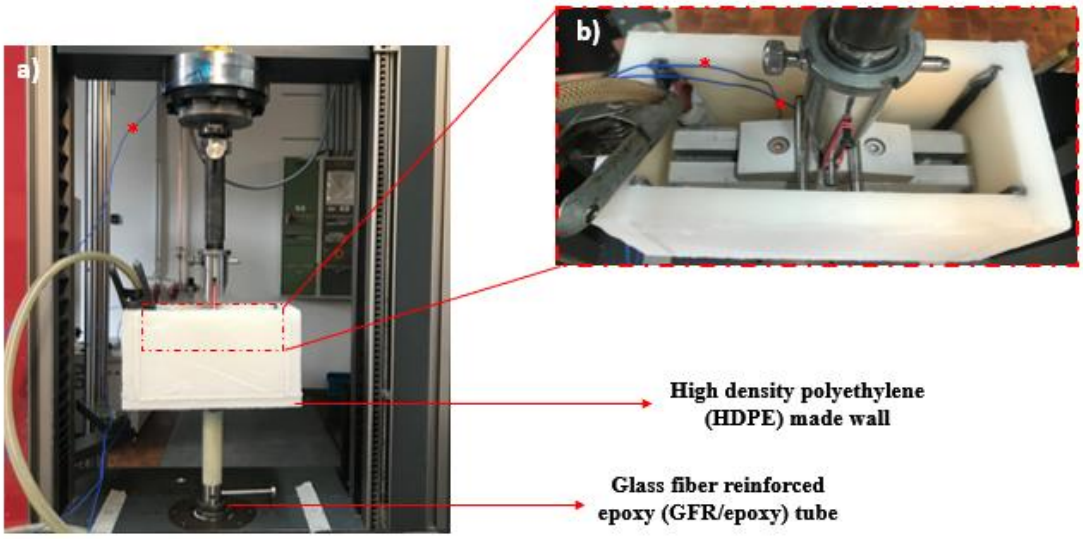

Figure 17: Single edge notched bending test set-up. The image a and b show the in-house built bucket and equipment construction from upside, respectively. Red asterisks depict the temperature measurement spots throughout the experiment.

The temperature data measurements were carried out through the 3-Channel Temperature Datalogger. Three cables were connected to the different parts of the test setup in which room temperature, the supporter of the mechanical test equipment and the bottom of the HDPE bucket as depicted in Figure 17.

2.4 Microscopy studies

Optical and scanning electron microscopy were used for the fracture surface analysis of the specimens after single-edge notched bending (SENB) testing. Cross-sectional analysis and measuring the depth of notch length of the specimens were observed in an optical microscopy together with the SEM.

2.4.1 Visual Light Microscopy (VLM)

Optical microscopy was performed using VHX-S650E, Keyence microscope to measure the notch length of the mechanically tested specimens and cross-sectional analysis of the modified epoxy. Thanks to this, fracture toughness and fracture energy values will be calculated. As can be seen in Figure 18, the red rectangle shows the cross-sectional area of the specimen after SENB test, and this area was observed via VLM. In the right-side image the red arrows present three different cut-

parts of the specimen, which are short, middle, and longest cuts, to measure the total notch length after cutting saw blade and razor blade, respectively.

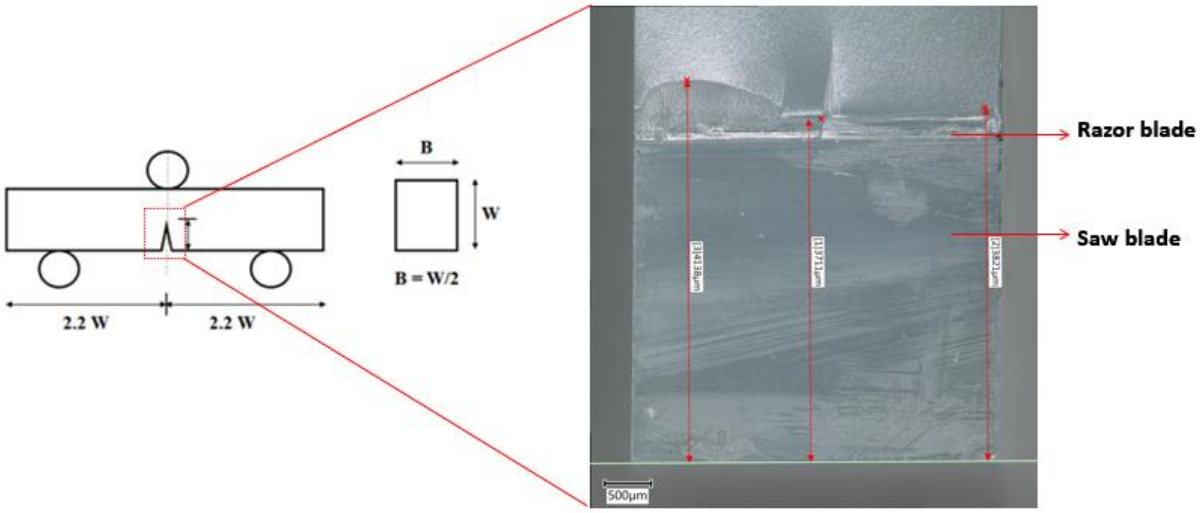

Figure 18: VLM image of a tested specimen and the red arrows depict the notch length.

2.4.2 Scanning Electron Microscopy (SEM)

The fracture surface analysis was studied using a scanning electron microscopy (Zeiss Leo Supra VP 35, SEM) at an accelerating voltage of 5 kV. All specimens were coated using gold-palladium (Au-Pd) sputter coater (SCD 050 from Baltec) with 40 mA voltage for 50 seconds to reduce the electron charging.

3 Results & Discussion

This section discusses all the findings from the previous parts of the thesis that helps answering the research questions.

3.1 Dynamic Mechanical Thermal Analysis (DMTA)

Dynamic mechanical thermal analysis (DMTA) was carried out using a Gabo Eplexor 500 N (NETZSCH GABO Instruments) DMTA machine at a fixed frequency of 1 Hz. The tests were performed over a temperature range between -150 °C and +150 °C with the heating rate of 2 K/min for each group. Specimens with the dimensions of 50 mm x 4mm x 7 mm were tested in tensile testing mode. To understand the Tg differences between the top and bottom parts of the manufactured specimens in case there is precipitation, two different parts of the specimen were observed in DMTA. The Tg values were measured from the largest peak of tan δ and are shown in Table 6 below. Additionally, the DMTA graphs for unmodified epoxy, core-shell, elastomer and carbon nanotube particle modified epoxy groups displayed in this chapter separately.

Table 6: Glass transition temperatures (Tg) of each group from DMTA results.

Specimen Group	Tg (°C) Top	Tg (°C) Bottom
Unmodified epoxy	104.5	104.5
10 wt % Polycavit 3565	103.6	103.5
20 wt % Polycavit 3565	98.7	100.5
20 wt % Polydis 3614	102.6	101
30 wt % Polydis 3614	99.7	99.9
0.3 wt % NC 7000	102.8	102.7

The Table 6 depicts that Tg value of the unmodified epoxy was measured as 104.5 °C, which shows any difference between up and bottom sides of the specimen. Moreover, it was observed that the addition of the particles into the epoxy resin does not substantially alter the glass transition value of the modified epoxy. Besides this, the addition of the core-shell, elastomer and carbon nanotube particles caused a small decrease on the Tg of the epoxy. Usually, Tg is taken as a god indicator of the degree of cross-linking in the epoxy matrices. Therefore, the constancy of Tg can be taken as the equal levels of cross linking in the unmodified or modified matrices. Hence, the addition of the particles to modify the epoxy resin has no changes on the crosslinking density of the system as reported in previous studies [67–69]. Moreover, testing the top and bottom sides of the particle loaded specimens showed that there are only minor changes due to a possible non-homogenous distribution of particles on the Tg value of the modified epoxy.

In addition to Table 6, Figure 19 shows the complex modulus E* of 10 wt.% Polycavit curves as calculated via DMTA, in relation to temperature. These results confirm that the glass transition temperature of the epoxy with the addition of 10 wt.% remained unchanged since the lines overlap with each other at around 100 °C which corresponds the Tg. It was found, at low temperature range which is between -150 – 0 °C, that an increase occurs in the complex modulus of the 10 wt.% Polycavit modified epoxy. This finding indicates that the presence of 10 wt.% Polycavit in the epoxy increases the brittleness of the modified epoxy.

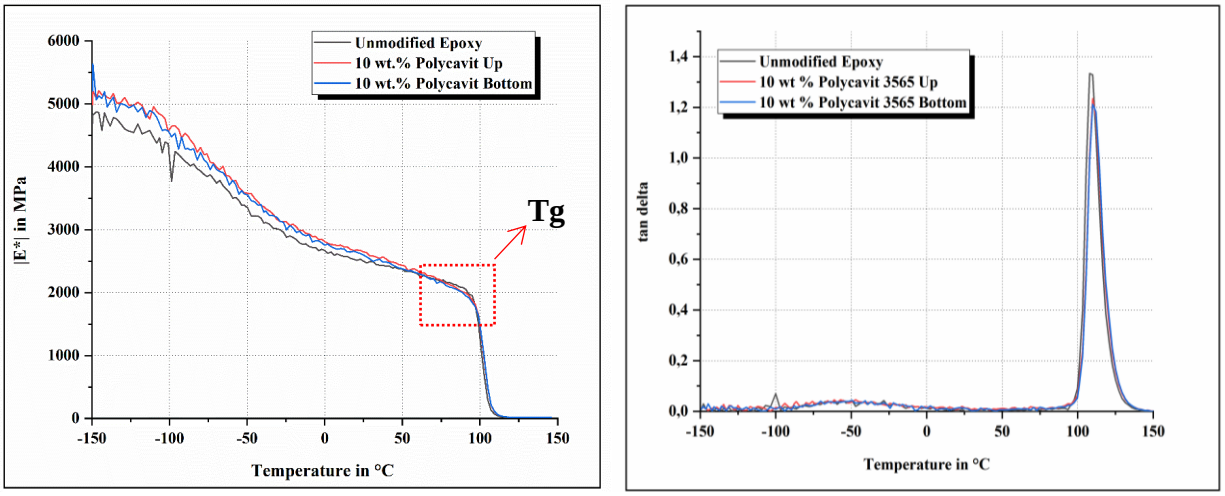

Figure 19: DMTA result for 10 wt.% Polycavit 3565.

On the contrary to Figure 19, Figure 20 shows a decrease on the complex modulus with the content of 20 wt.% Polycavit in the epoxy resin. This is the indication of that increasing the core-shell content decreased the brittleness of the modified epoxy at low temperature conditions. Furthermore, it can be seen that there is no changes on the glass transition temperature of the 20 wt.% Polycavit modified epoxy. Moreover, it is noteworthy to mention that the top and the bottom sides of the core-shell particles in the modified epoxy resin exhibited nearly the same complex modulus values.

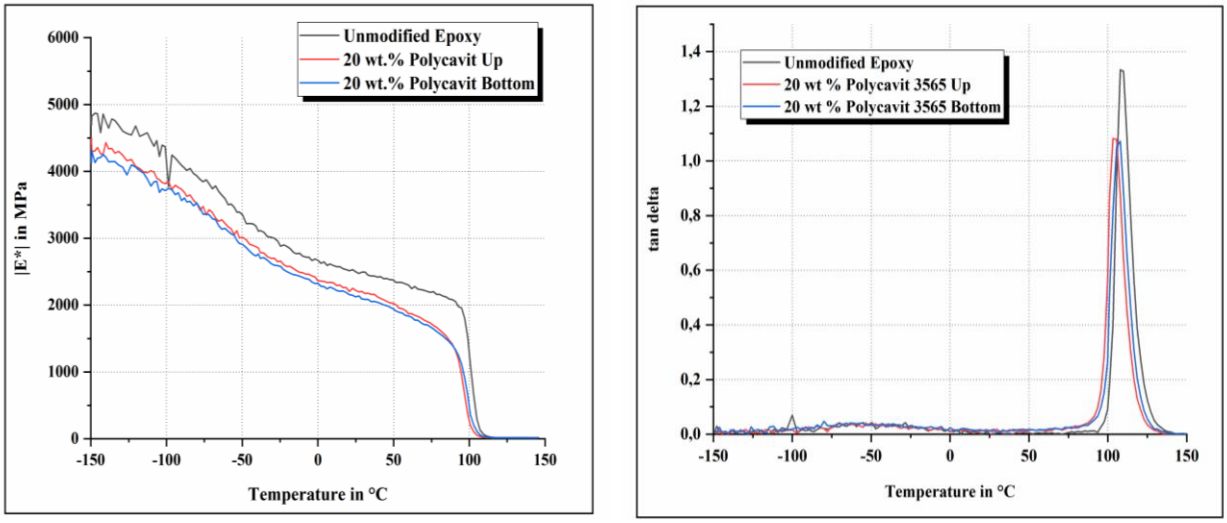

Figure 20: DMTA result for 20 wt.% Polycavit 3565.

Similarly, the addition of the elastomer particles proved that the presence of 20 wt.% and 30 wt.% Polydis did not change the glass transition temperature of the modified epoxy as seen in Figure 21 and Figure 22. In Figure 21, the addition of the 20 wt.% Polydis particles at the bottom part was found to decrease the brittleness of the modified epoxy at low temperature whereas the up part of the elastomer particle modified epoxy exhibited nearly the same value with the unmodified epoxy resin system.

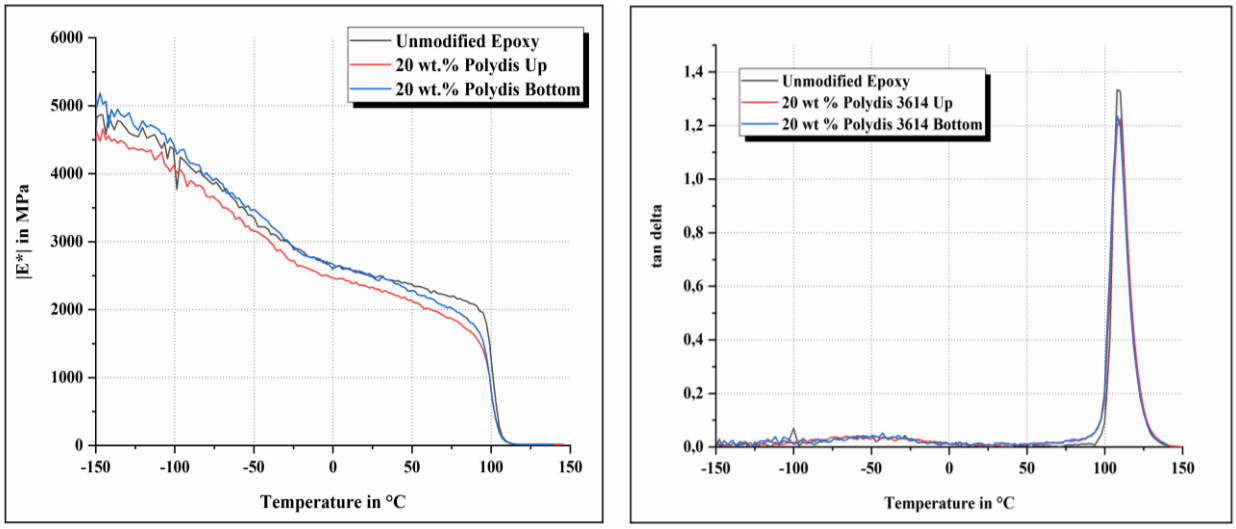

Figure 21: DMTA result for 20 wt.% Polydis 3614.

As seen in Figure 22, an increase in content ratio of elastomer particles indicated a decrease the complex modulus value in comparison to unmodified epoxy system. In relation to content ratio in elastomer particles, higher amount of elastomer particles in the epoxy resin decreased the brittleness of the modified epoxy at low temperature conditions.

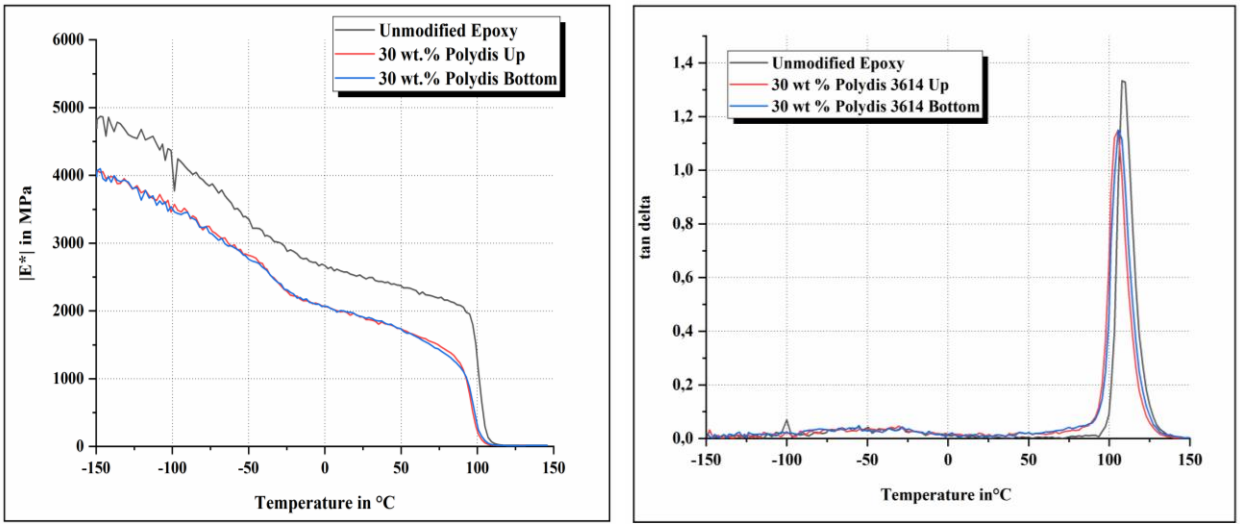

Figure 22: DMTA result for 30 wt.% Polydis 3614.

These results show that the soft rubbery particles make the comparatively rigid epoxy matrix less stiff, which is expected and consistent with other researchers' findings [32,34,70].

In the case of the carbon nanotube added epoxy systems, there was also significant difference in complex modulus values between unmodified and 0.3 wt.% MWCNT modified epoxy resin as seen in Figure 23-left. Moreover, it is worth to mention that the differences in complex modulus at low temperature conditions between top and bottom parts of the specimens showed distinctly low values. Such differences are believed to exist due to the absence of the carbon nanotube particles at the top parts of the 0.3 wt.% NC 7000 modified epoxy due to the precipitation of the particles under the effects of gravitational force during curing. On the other hand, 0.3 wt.% carbon nanotube did not alter the glass transition temperature of the modified epoxy system as seen n Figure 23-right.

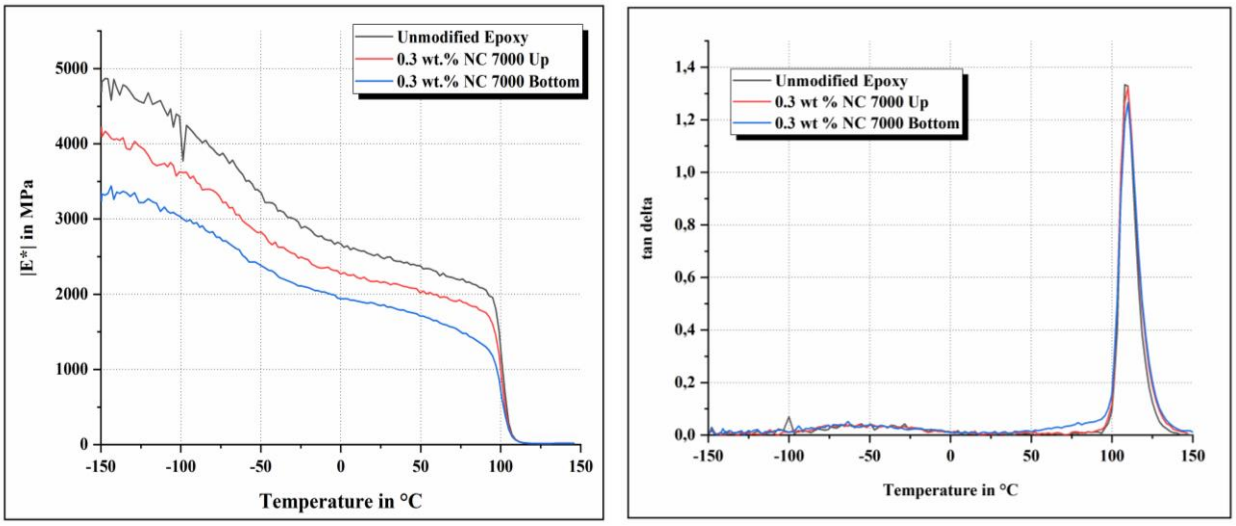

Figure 23: DMTA results for 0.3 wt.% NC 7000.

Figure 24 provides the comparative results of core-shell and elastomer particles with the filler content ratio in the epoxy resin as well as carbon nanotube. Using the same amount but different filler in the epoxy resin indicated that although they both influence on the complex modulus, the complex modulus of both modified matrices was below the complex modulus value of unmodified epoxy, among the particle modified matrices 20 wt.% core-shell showed less brittleness than 20 wt.% elastomer in the modified epoxy system.

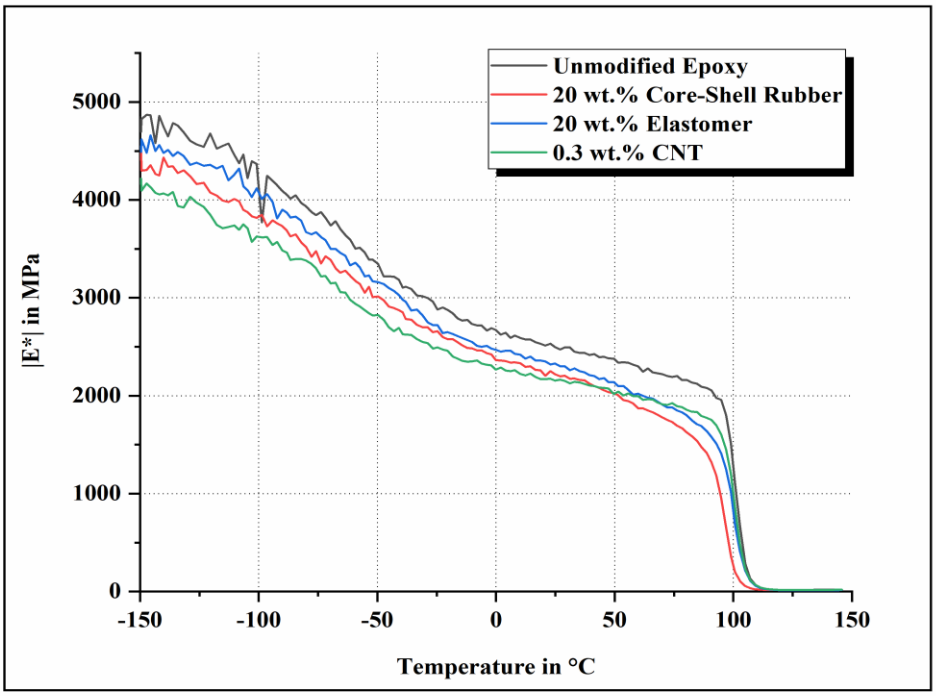

Figure 24: DMTA results for 20 wt.% core-shell particles, 20 wt.% elastomer and 0.3 wt.% MWCNT modified epoxy.

3.2 Single-Edge Notched Bending (SENB) Test

Five specimens at least for each group were tested for single-edge notched bending of both the bulk and the particle modified epoxies as required in the standard [66]. The mechanical tests were conducted under different temperature conditions which are room temperature, -40 °C and -80 °C. The fracture toughness, K_{1c}, was calculated as

$$K_{1c} = \left(\frac{P_Q}{BW^{\frac{1}{2}}}\right) f(x) \tag{3.1}$$

f(x) is described in Equation 2.2.

where P_Q is maximum load, B and W specimen thickness and width, respectively.

and the fracture energy, Gıc, calculated as

$$G\imath c = \frac{(1 - v^2)K\imath c^2}{E} \tag{3.2}$$

where v is poisson ratio that is extracted from the literature for epoxy resin which corresponds 0.34 [71] and E is Young's modulus that is obtained from dynamic mechanical thermal analysis (DMTA) results. The calculation results for fracture toughness and fracture energy were reported as seen Table 7 and Table 8 and shown in the following graphs in this section.

Table 7: Fracture toughness [MPa.m$^{1/2}$] values of each group at different temperature conditions.

Specimen	Room Temperature	-40 °C	-80 °C
Neat	0.99 ± 0.35	1.22 ± 0.24	1.30 ± 0.15
0.3 wt.% CNT	1.07 ± 0.27	1.31 ± 0.27	1.73 ± 0.23
10 wt.% Core-Shell	1.12 ± 0.22	1.17 ± 0.14	1.25 ± 0.26
20 wt.% Core-Shell	1.46 ± 0.11	1.36 ± 0.15	1.56 ± 1.12
20 wt.% Elastomer	1.70 ± 0.08	1.23 ± 0.22	1.58 ± 0.09
30 wt.% Elastomer	1.73 ± 0.11	2.17 ± 1.84	1.77 ± 0.07

As seen in Table 7, the value of Kıc was found to improve with 30 wt.% elastomer particle content from 0.9 MPa.m$^{1/2}$ up to 1.73 MPa.m$^{1/2}$ at room temperature. Figure 25, 20 wt.% and 30 wt.% content ratios of elastomer in the epoxy resin system showed that they have the highest fracture toughness values in comparison to other groups at room temperatures. On the other hand, 20 wt.% addition of core-shell particles displayed that it increases the fracture toughness whereas 10 wt.% core-shell modified epoxy shows minor changes in fracture toughness in comparison to the unmodified epoxy. Moreover, 0.3 wt.% carbon nanotube added epoxy resins fracture toughness enhanced from 0.99 to 1.07 MPa.m$^{1/2}$. However, as can be seen in Figure 25, addition of 0.3 wt.% CNT did not significantly influence Kıc in comparison to 20 wt.% core-shell, 20 wt.% and

30 wt.% elastomer particle addition. Also, it is worth to notice that 10 wt.% core-shell and 0.3 wt.% CNT added epoxy systems had nearly the same values which are 1.07 and 1.23 MPa.m$^{1/2}$, respectively, in Kıc at room temperature conditions. At room temperature, a conclusion can be made is that adding elastomer particles into the epoxy resin works better than other modified epoxy groups.

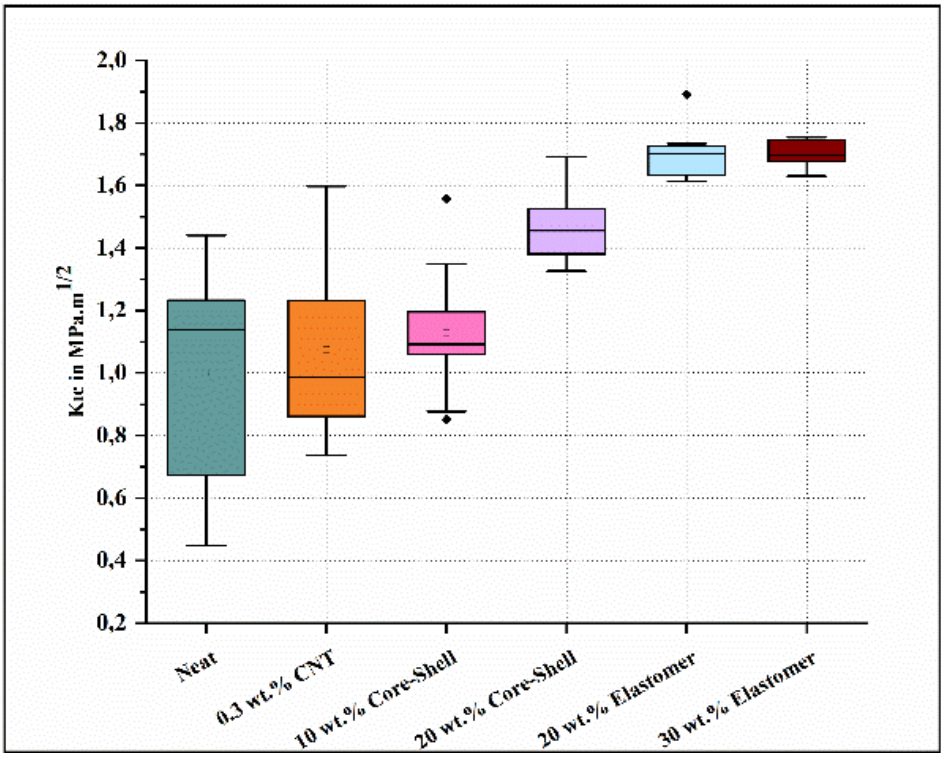

Figure 25: Fracture toughness for the modified and unmodified epoxy at room temperature.

On the other hand, for -40 °C temperature condition, the fracture toughness of the unmodified epoxy increased from 1.22 MPa.m$^{1/2}$ to 1.31 MPa.m$^{1/2}$ with the addition of 0.3 wt.% CNT. Addition of 10 wt.% core-shell particle into the epoxy resin reduced the fracture toughness at -40 °C whereas 20 wt.% core-shell particle modified epoxy showed minor changes. That means 10 and 20 wt.% core-shell particles did not influence the fracture toughness at -40 °C. Besides this, 20 wt.% elastomer modified epoxy indicated the same value as the unmodified epoxy. In this case, 20 wt.% addition of different particles (the same particle content but different particles), core-shell relatively works better than elastomer modified epoxy systems as can be seen in Figure 26. On the contrary, 30 wt.% elastomer modified epoxy exhibited the highest value in Kıc in comparison to other batches. For -40 °C, 30 wt.% addition of the epoxy resin showed higher resistance to crack propagation than modified epoxy groups.

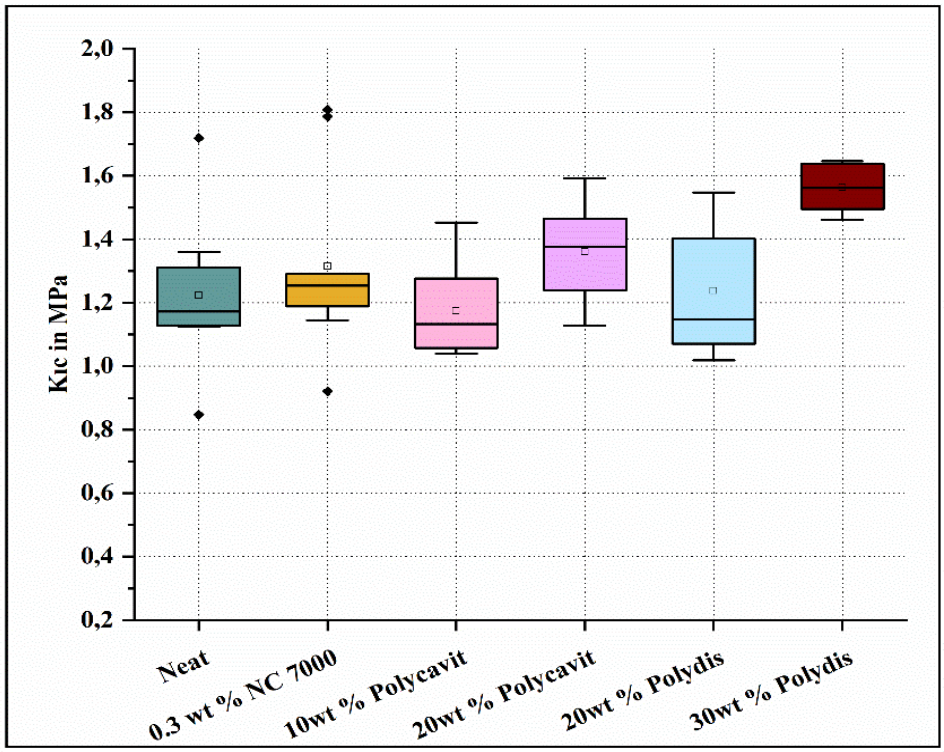

Figure 26: Fracture toughness for the modified and unmodified epoxy at -40 °C.

For -80 °C, it has been noticed that addition of 10 wt.% core-shell particles decreased the fracture toughness from 1.30 MPa.m$^{1/2}$ to 1.25 MPa.m$^{1/2}$ while increasing the filler content up to 20 wt.% showed higher toughness values. On the other hand, using the same filler content (20 wt.% elastomer and 20 wt.% core-shell) but different particles displayed that they behaved nearly the same at -80 °C. Moreover, these two filler contents, which are core-shell and elastomer, showed that the fracture toughness of the modified epoxy increased from 1.30 to 1.56 MPa.m$^{1/2}$ and 1.58 MPa.m$^{1/2}$, respectively as seen in Table 7. 30 wt.% elastomer modified epoxy showed the highest fracture toughness value at -80 °C. It can be said that addition of 30 wt.% elastomer fillers into the epoxy resin exhibits highest fracture toughness values at all different temperature conditions. For the 0.3 wt.% carbon nanotube modified epoxy resin at -80 °C, the results say that presence of carbon nanotube enhanced the fracture toughness. Exceptionally, 0.3 wt.% carbon nanotube worked better than other temperature conditions (room temperature and -40 °C). This situation can be explained based on the literature values of thermal expansion coefficient, which is 45 to 55 × 10^{-6}/K [72] for the neat epoxy that is greater than the multi walled carbon nanotube (MWCNT) which is 2.1^{-5}/K [73]. That means when the temperature is lower, the epoxy resin contracts more than the MWCNTs and therefore there will be a compact cohesion between the epoxy and the carbon nanotube. Throughout the mechanical tests at -80 °C, the crack needed more energy to propagate along the trajectory and hence the effect of the temperature on the toughening performance of the 0.3 wt.% MWCNT epoxy resin showed higher values in both the fracture toughness and the fracture energy that will be discussed further in the coming sections.

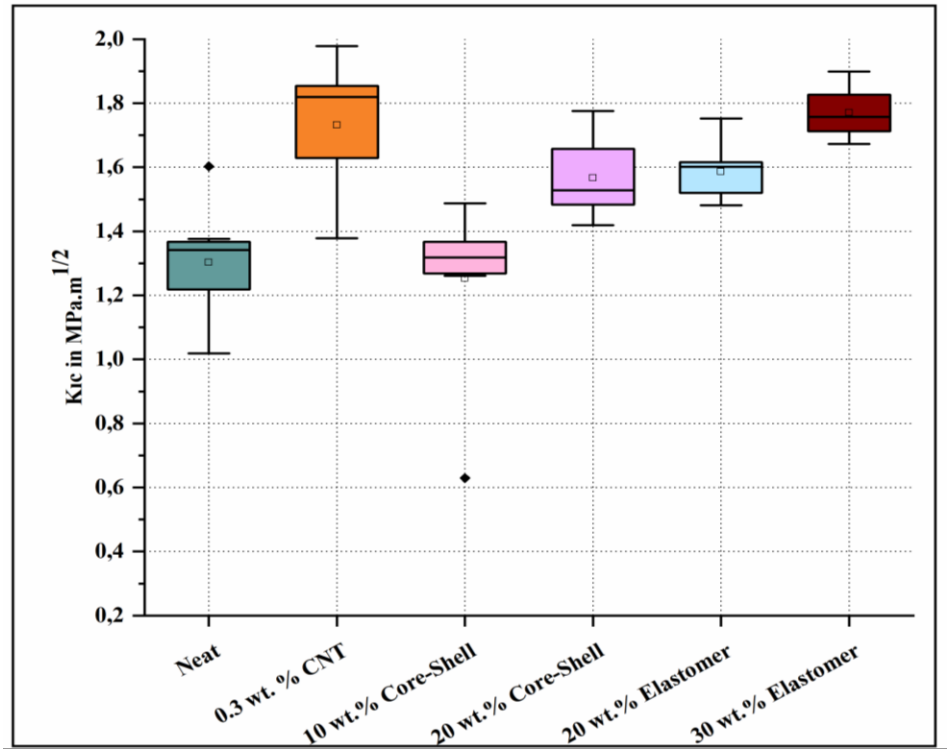

Figure 27: Fracture toughness for the modified and unmodified epoxy at -80 °C.

In Table 8 it summarizes the fracture energy values of the toughened epoxy at different temperature conditions. At room temperature, it was found that fracture energy, GIc, improved with the presence of 30 wt.% elastomer particles from 416 to1475 kJ/m^2, which means elastomer modified epoxy needs more energy to break the specimens at ambient temperature.

Table 8: Fracture energy [kJ/m^2] values of each group at different temperature conditions.

Specimen	Room Temperature	-40 °C	-80 °C
Neat	416 ± 249	461 ± 194	414 ± 97
0.3 wt.% CNT	529 ± 276	642 ± 282	957 ± 246
10 wt.% Core-Shell	458 ± 184	385 ± 98	359 ± 118
20 wt.% Core-Shell	898 ± 148	610 ± 134	650 ± 102
20 wt.% Elastomer	1065 ± 113	492 ± 167	589 ± 68
30 wt.% Elastomer	1475 ± 207	849 ± 80	910 ± 79

Furthermore, the effect of the presence of both 0.3 wt.% CNT and 10 wt.% core-shell did not improve the fracture energy of the particle modified epoxy in comparison to other batches as can be seen in Figure 28. However, increasing the filler content in the epoxy resin indicated the higher fracture energy values for both core-shell and elastomer particles.

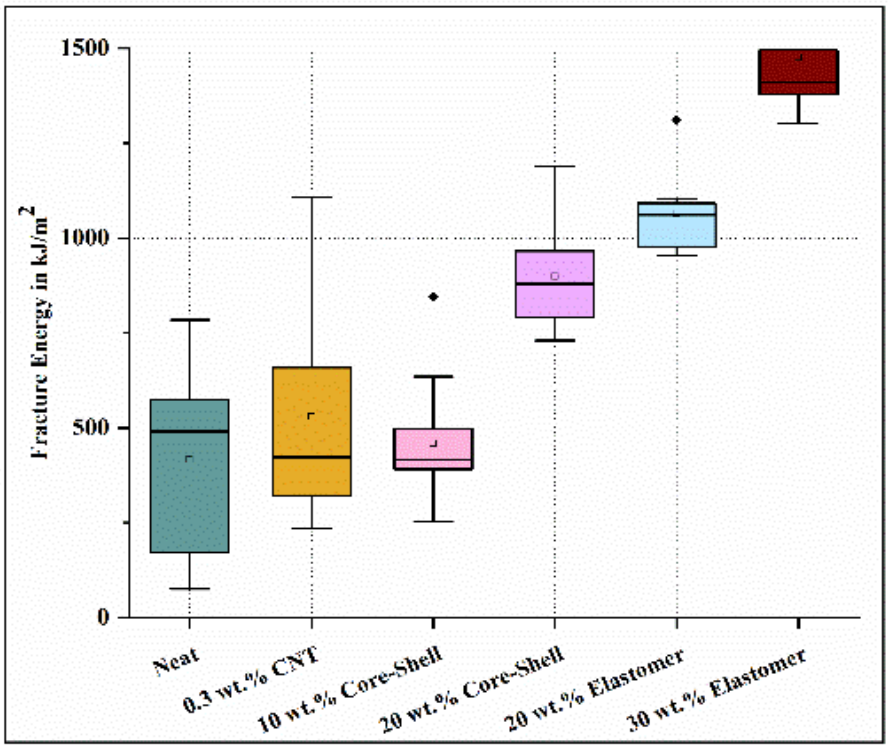

Figure 28: Fracture energy for the modified and modified epoxy at room temperature.

Likewise, the fracture energy at -40 °C was improved to a higher value with the addition of 30 wt.% elastomer as given in Figure 29. However, the temperature effect on the fracture energy values of the 0.3 wt.% MWCNT modified epoxy showed that it has a higher fracture energy than room temperature due to the different thermal expansion coefficient values. Also, it is worthy to point out that epoxy matrices with the same content concentration of elastomer and core-shell (20 wt.%) exhibited different fracture energies. In this case, 20 wt.% core-shell particles illustrated a stronger interaction between the particles and the epoxy resin than the elastomer additives.

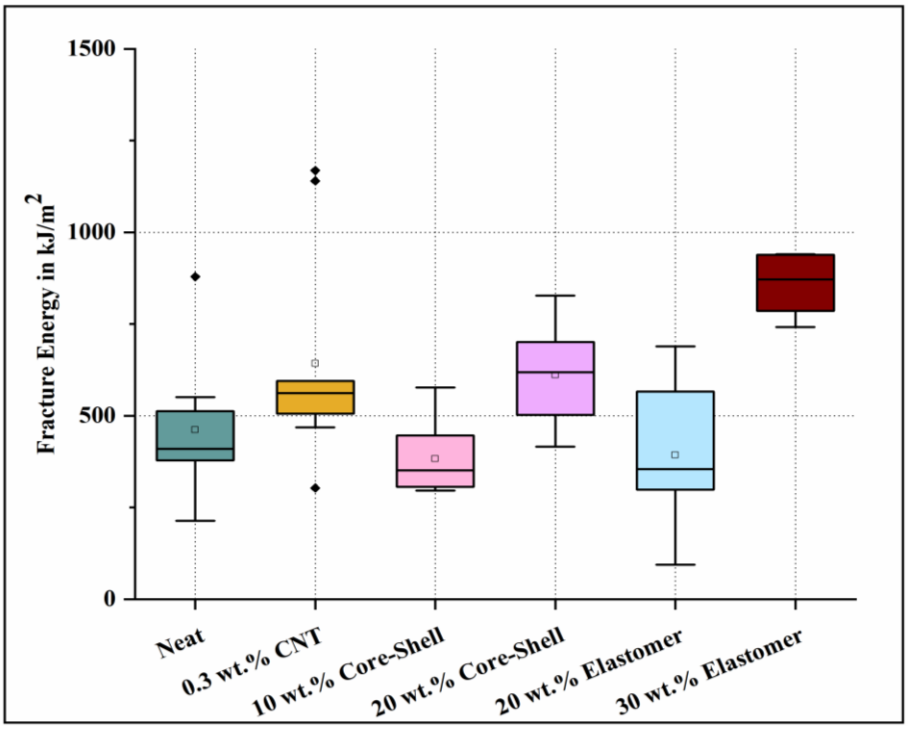

Figure 29: Fracture energy for the modified and modified epoxy at -40 °C.

Comparatively, at -80 °C, the toughening performance of 0.3 wt.% MCNT epoxy appeared notably bigger than other groups.

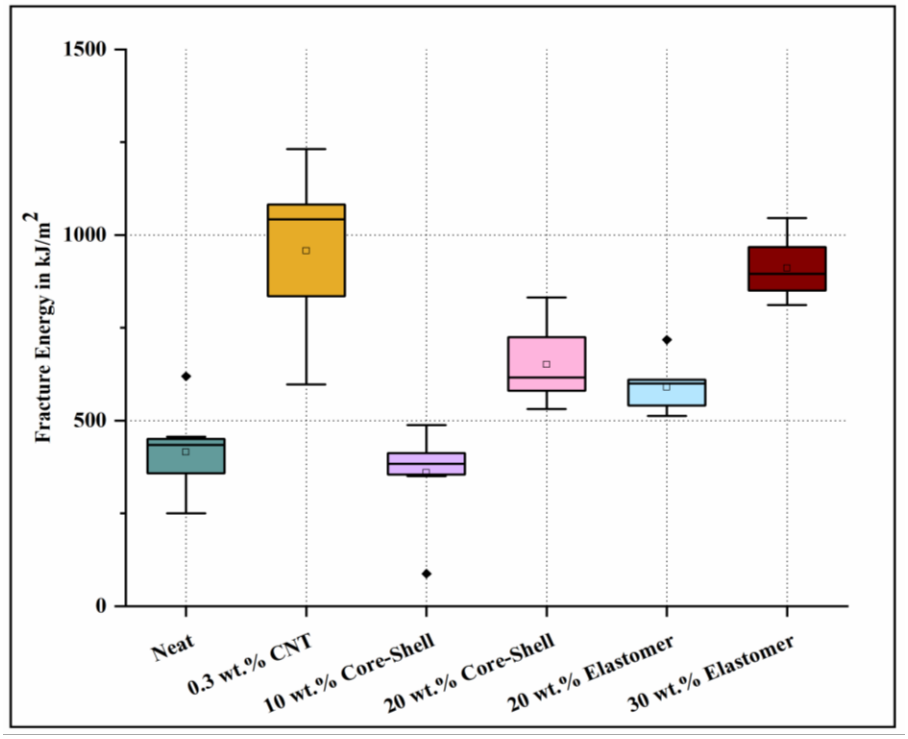

Figure 30: Fracture energy for the modified and modified epoxy at -80 °C.

Besides, the toughening effect on higher filler concentration of the elastomer particles worked better at this temperature condition. However, the fracture energy of the 10 wt.% core-shell did not work well, which shows lower value than the unmodified epoxy. This may be explained by that the interaction between 10 wt.% core-shell and the epoxy was not sufficient to withstand crack propagation due to the lack of adequate amount of the core-shell particles. From the fracture energy values at -80 °C, in terms of the same filler content amount but different type of fillers, 20 wt.% core-shell had a higher resistance against crack propagation at this temperature, as well as -40 °C. To put in numbers, the fracture energy ascended from 414 to 650 kJ/m^2 for 20 wt.% core-shell modified resin.

3.3 Scanning Electron Microscopy (SEM)

The fracture surfaces of the unmodified and modified epoxies were studied using scanning electron microscopy after SENB tests. All SEM observations will be discussed in detail to further evaluate the mechanical tests of the modified epoxy resins for different temperature values.

Figure 31 shows that there is no obvious feature except several forkings on the surface of the SENB tested modified epoxy at room temperature. It was smooth and glassy as already investigated in the previous studies [74]. Also, it was discovered that there was no large-scale plastic deformation on the surface for brittle thermosetting polymers [75].

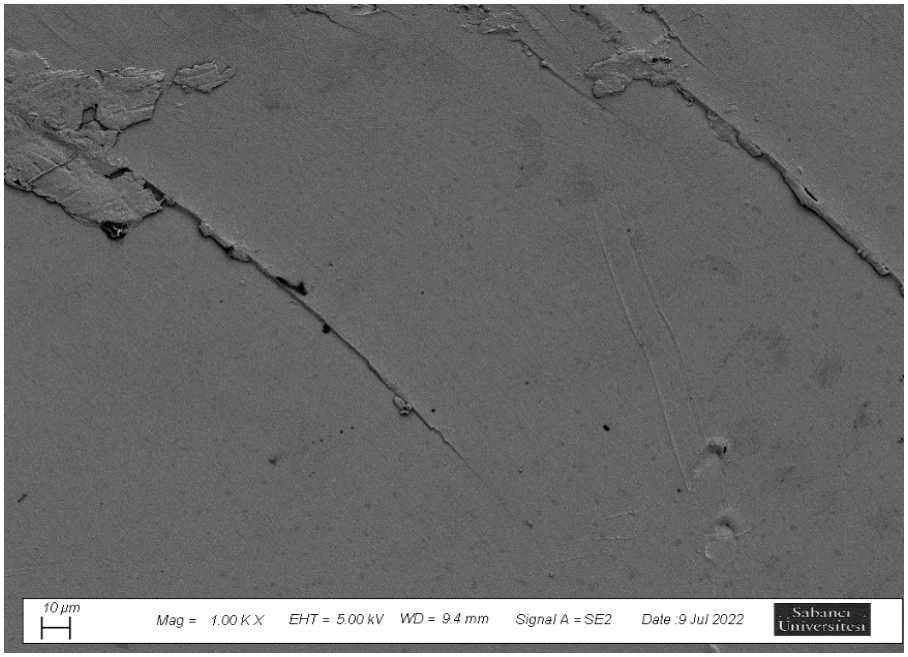

Figure 31: SEM image of the fracture surface of the unmodified epoxy. The crack direction was indicated by the arrow.

Figure 32 depicts that different fracture surfaces of the core-shell modified epoxy at different filler content concentrations. In these images, crack forkings and flow lines are significant and there is a rough surface in comparison to the unmodified epoxy resin. It was found that partial cavitations

were present in the core-shell particle modified epoxy. This phenomenon was also observed the core-shell particle modified epoxies that had been already investigated by other researchers [76–79]. They emerged from the internal cavitation.

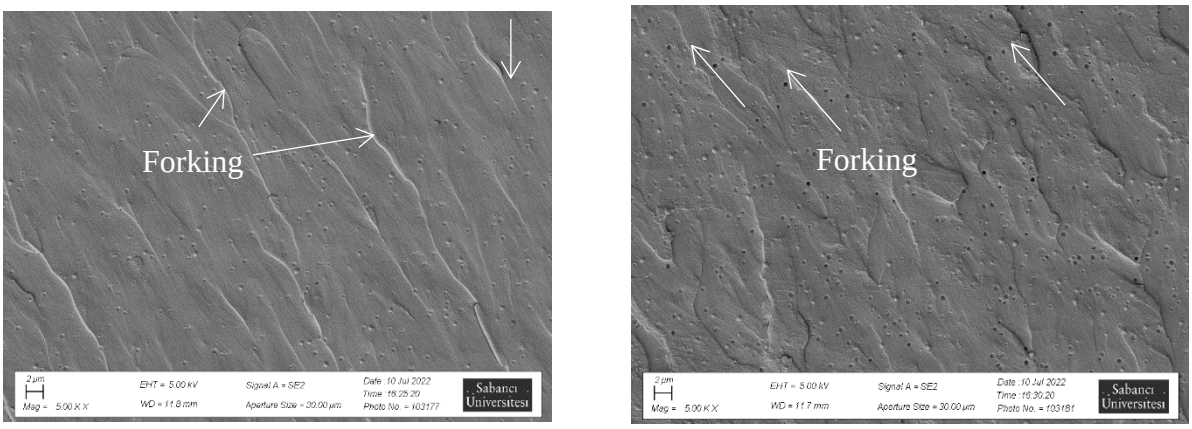

Figure 32: SEM image of the fracture surface of the (left) 10 wt.% core-shell and (right) 20 wt.% core-shell epoxy. The crack direction was indicated by the arrow.

Figure 33 presents the elastomer modified epoxy after SENB tests. In the left picture which shows 20 wt.% elastomer, the crack trajectory changed the direction from the beginning of the crack due to the presence of the elastomer particles. To distinguish the difference between the modified and the elastomer particle modified epoxies, this image is the concrete proof of the influence of elastomer additives in the epoxy resin. The fracture surface was found rough and there were no smooth surfaces. In both images, feather markings because of the repeated crack forkings were observed due to the exceeding energy. Moreover, those crack forkings and feathers, as well as other features, were caused extensive fracture energy in the modified epoxy resin. Hence, those images were the evidence that a higher fracture energy was needed to propagate the crack and scanning electron microscopy images verified the obtained for data.

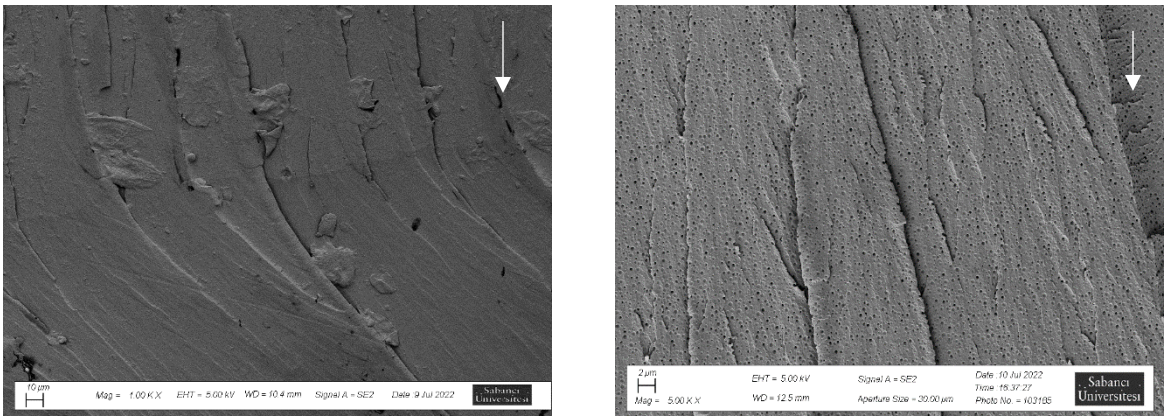

Figure 33: SEM image of the fracture surface of the (left) 20 wt.% elastomer and (right) 30 wt.% elastomer epoxy. The crack direction was indicated by the arrow.

In Figure 34, likewise, the 30 wt.% elastomer modified epoxy showed that it illustrated void growth on the fracture surface as it was found at ambient temperature, as well. These voids can be explained by the presence of the cavitations, that form void growth throughout the mechanical tests.

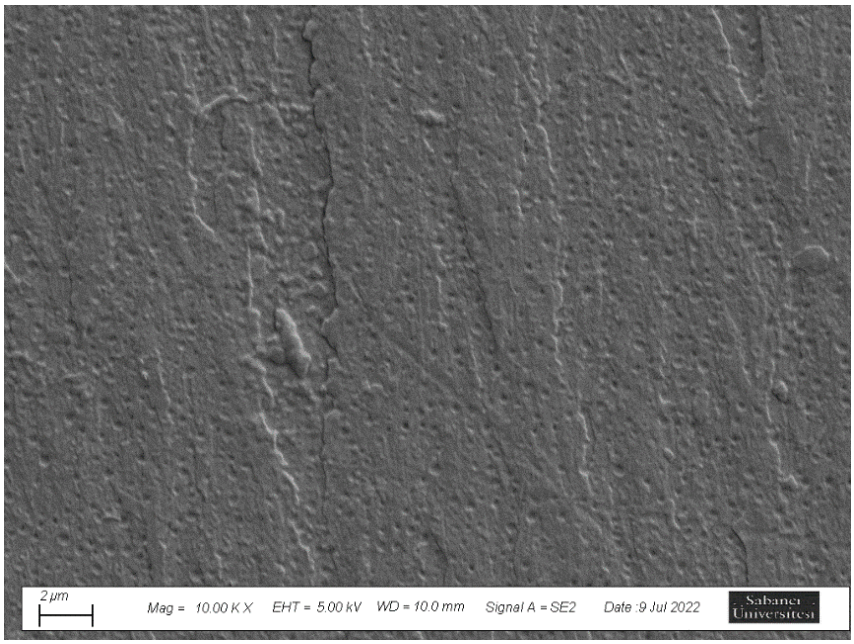

Figure 34: SEM image of the fracture surface of the 30 wt.% elastomer epoxy at -80 °C.

The effect of different particle diameters on the mechanical behavior of the modified epoxies at different temperatures were not investigated due to the lack of time. The study needs more comprehensive investigation to clarify the effect of particle diameter. It is highly likely that particles of different diameter can have different effects on mechanical properties and this influence can vary with temperature. This is suggested as a future study plan. The same interpretation might be valid for the core-shell particle modified epoxy since it has been already studied by different researchers [1].

Figure 35 exhibits the 0.3 wt.% MWCNT epoxy resin. As can be seen in the left image, the fracture surface of the crack initiation area showed rough surfaces as well as many flow lines. Those flow lines generated crack propagation at different locations. This situation, which is peculiar to the brittle materials, also matches up with the literature [80]. Moreover, in the left image, it was clearly observed that white particles, which are shown the red circles, represent the nanotube pull out and debonding. Hence, because of the debonding, void growth generated between the MWCNT and the epoxy resin, followed by the plastic deformation.

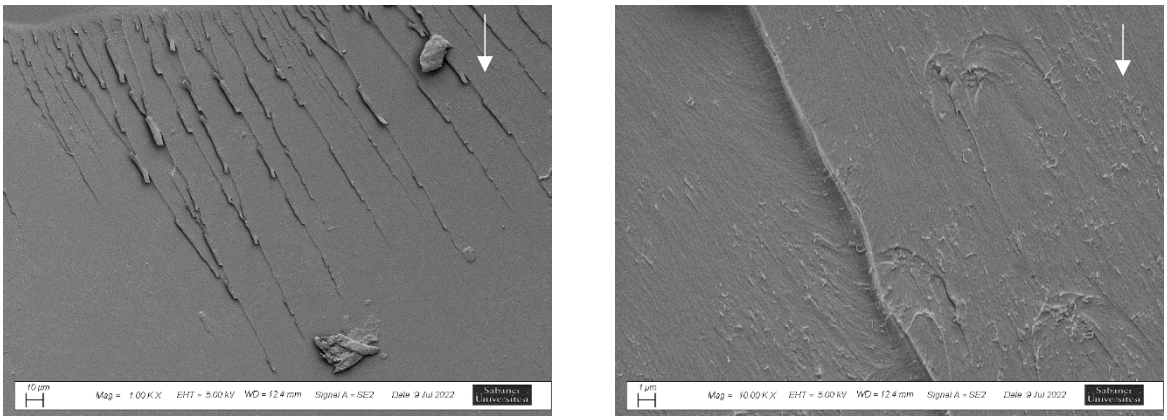

Figure 35: SEM image of the fracture surface of the 0.3 wt.% MWCNT at -40 °C. Left and right images show lower and higher magnification images, respectively. The crack direction was indicated by the arrow.

4 Conclusion

The goal of this thesis was to enhance the fracture toughness mechanism of the modified epoxy resin at low temperature environments and to examine the potentials of different additives which were blended in the epoxy resin. For this aim, three different epoxy systems (core-shell, elastomer particles and multi-walled carbon nanotube (MWCNT)) were identified in this study, and following this, mechanical performance of the modified epoxies were carried out at room temperature, -40 °C and -80 °C, in order to evaluate their performance. The toughenability of the epoxy was studied according to the fracture toughness, the thermal-mechanical analysis (DMTA) results and the fractography.

To this end, these results led to four main findings which were drawn from this study:

- The glass transition temperature (Tg) of the unmodified epoxy was 104.5 °C. The addition of three different additives did not strongly alter the measured Tg value. However, it was found that the modified epoxy exhibited less brittleness at lower temperature conditions withing the range of the DMTA test parameter.

- Using different filler content had an effect on the fracture behavior of the modified epoxy. Increasing the content ratios of core-shell and elastomer particles resulted that fracture toughness and fracture energy values were enhanced with the addition of these agents in the epoxy resin at all temperature conditions.

- Each toughener mechanism had their own influence in fracture toughness of the modified epoxy system. 30 wt.% elastomer modified epoxy exhibited highest fracture toughness behavior in comparison to other batches at every temperature environment. Furthermore, the unmodified epoxy presented the lowest fracture toughness value at each temperature condition. The morphology of the unmodified epoxy was found uniform, no more features, whereas the modified epoxy groups displayed crack forkings, cavitations, debonding mechanisms on the surfaces. These morphological results confirmed that the modified epoxy systems absorbed more energy for crack propagation due to the presence of the additives.

- The execution of the SENB tests at different temperature environments which were ambient, -40 °C and -80 °C revealed that 30 wt.% elastomer increased the fracture energy from 414 kJ/m^2 to 910 kJ/m^2 at -80 °C. Moreover, the presence of 0.3 wt.% MWCNT enhanced the fracture energy from 414 kJ/m^2 to 957 kJ/m^2 which was the highest at the same temperature condition.

5 Recommendation

This thesis focused on further understanding of the modified epoxy's fracture behavior at different temperature situations and also, studied finding the proper additive and the additive amount. The findings gave a better understanding of the modified epoxy's fracture energy in SENB test process. However, further investigation is needed to find out the carbon fiber reinforced polymer materials' behavior for deeper understanding of cryogenic fuel tank materials. Several future work recommendations for the improvement of this technology are given:

- Throughout this thesis, only limited amount of the fillers was used. For MWCNT and elastomer, the only amount was 0.3 wt.% and 30 wt.%, respectively. These ratios exhibited better mechanical results at the lowest temperature. For future studies, higher amount should be tried to see the filler content effect on fracture energy. The same interpretation can be said for core-shell particles since only 10 wt.% and 20 wt.% amount was done during the overall experimental process.

- After finding the proper amounts which will work better at lower temperatures for each group, various combinations of toughening agents should be tried for the enhancement of the fracture toughness.

- Further understanding of the lower temperature conditions is required to test the new specimens to see the differences in this investigation. Due to the limited time and the limited test equipment, the lowest temperature was set for -80 °C and by lowering the temperature conditions new finding should be considered.

- Research on the addition of carbon fibers which can be used for hydrogen fuel vessel material should be investigated after improving the matrix materials with respect to the given recommendations. The CFRPs with the improved matrix which consists of the proper amount of fillers can be tested at cryogenic temperature environments for storing liquid hydrogen technology to develop new material which will withstand above-mentioned conditions.

6 References

[1] J. Chen, Toughening Epoxy Polymers and Carbon Fibre Composites with Core-Shell Particles, Block Copolymers and Silica Nanoparticles, Imperial College London, 2013.

[2] G. Tesoro, Epoxy resins-chemistry and technology, 2nd Edition, Clayton A. May, Ed., Marcel Dekker, New York, 1988, 1,288 pp. Price: $195.00, J. Polym. Sci. B Polym. Lett. Ed. 26 (1988) 539. https://doi.org/10.1002/pol.1988.140261212.

[3] K. Whitley, T. Gates, Thermal/Mechanical Response and Damage Growth in Polymeric Composites at Cryogenic Temperatures, in: 43rd AIAA/ASME/ASCE/AHS/ASC Structures, Structural Dynamics, and Materials Conference, Denver, Colorado, American Institute of Aeronautics and Astronautics, Reston, Virigina, 04222002.

[4] V.T. Bechel, J.D. Camping, R.Y. Kim, Cryogenic/elevated temperature cycling induced leakage paths in PMCs, Composites Part B: Engineering 36 (2005) 171–182. https://doi.org/10.1016/j.compositesb.2004.03.001.

[5] W. Liu, S.V. Hoa, M. Pugh, Organoclay-modified high performance epoxy nanocomposites, Composites Science and Technology 65 (2005) 307–316. https://doi.org/10.1016/j.compscitech.2004.07.012.

[6] J. KIM, C. BAILLIE, J. POH, Y. MAI, Fracture toughness of CFRP with modified epoxy resin matrices, Composites Science and Technology 43 (1992) 283–297. https://doi.org/10.1016/0266-3538(92)90099-O.

[7] V.T. Bechel, M.B. Fredin, S.L. Donaldson, R.Y. Kim, J.D. Camping, Effect of stacking sequence on micro-cracking in a cryogenically cycled carbon/bismaleimide composite, Composites Part A: Applied Science and Manufacturing 34 (2003) 663–672. https://doi.org/10.1016/S1359-835X(03)00054-X.

[8] J.F. Timmerman, M.S. Tillman, B.S. Hayes, J.C. Seferis, Matrix and fiber influences on the cryogenic microcracking of carbon fiber/epoxy composites, Composites Part A: Applied Science and Manufacturing 33 (2002) 323–329. https://doi.org/10.1016/S1359-835X(01)00126-9.

[9] W.L. Tsang, A.C. Taylor, Fracture and toughening mechanisms of silica- and core–shell rubber-toughened epoxy at ambient and low temperature, J Mater Sci 54 (2019) 13938–13958. https://doi.org/10.1007/s10853-019-03893-y.

[10] F.D. Rossini, Report on International Practical Temperature Scale of 1968, The Journal of Chemical Thermodynamics 2 (1970) 447–459. https://doi.org/10.1016/0021-9614(70)90096-0.

[11] W. Xu, Q. Li, M. Huang, Design and analysis of liquid hydrogen storage tank for high-altitude long-endurance remotely-operated aircraft, International Journal of Hydrogen Energy 40 (2015) 16578–16586. https://doi.org/10.1016/j.ijhydene.2015.09.028.

[12] G. Babac, A. Sisman, T. Cimen, Two-dimensional thermal analysis of liquid hydrogen tank insulation, International Journal of Hydrogen Energy 34 (2009) 6357–6363. https://doi.org/10.1016/j.ijhydene.2009.05.052.

[13] S. GURSU, M. LORDGOOEI, S. SHERIF, T. VEZIROGLU, An optimization study of liquid hydrogen boil-off losses, International Journal of Hydrogen Energy 17 (1992) 227–236. https://doi.org/10.1016/0360-3199(92)90131-F.

[14] G. Petitpas, Simulation of boil-off losses during transfer at a LH2 based hydrogen refueling station, International Journal of Hydrogen Energy 43 (2018) 21451–21463. https://doi.org/10.1016/j.ijhydene.2018.09.132.

[15] S. Mital, J. Gyekenyesi, S. Arnold, R. M. Sullivan, J. Manderscheid, P. Murthy, Review of current state of the art and key design issues with potential solutions for liquid hydrogen cryogenic storage tank structures for aircraft applications, Engineering (2006).

[16] A.J. Kinloch, R.D. Mohammed, A.C. Taylor, C. Eger, S. Sprenger, D. Egan, The effect of silica nano particles and rubber particles on the toughness of multiphase thermosetting epoxy polymers, J Mater Sci 40 (2005) 5083–5086. https://doi.org/10.1007/s10853-005-1716-2.

[17] F. Hübner, A. Brückner, T. Dickhut, V. Altstädt, A. Rios de Anda, H. Ruckdäschel, Low temperature fatigue crack propagation in toughened epoxy resins aimed for filament winding of type V composite pressure vessels, Polymer Testing 102 (2021) 107323. https://doi.org/10.1016/j.polymertesting.2021.107323.

[18] P.K. Mallick, Fiber-reinforced composites: Materials, manufacturing, and design, third. ed., CRC Press, Boca Raton, Fla., 2008.

[19] J.-P. Pascault, R.J.J. Williams, General Concepts about Epoxy Polymers, in: J.-P. Pascault, R.J.J. Williams, R.J.J. Williams (Eds.), Epoxy polymers: New materials and innovations, Wiley-VCH, Weinheim, 2010, pp. 1–12.

[20] E.M. Petrie, Epoxy adhesive formulations: Epoxy properties and characteristics ; techniques for improving epoxy strength, flexibility, and durability ; testing and quality control guidelines, McGraw-Hill, New York, NY, London, 2006.

[21] A.S. Dunn, Polymer chemistry: An introduction (2nd edition) M. P. Stevens, Oxford University Press, New York, 1990. pp. xvii + 633, price £40 (hardback), £17.50 (paperback) ISBN 0-19-505759-7 (hardback) ISBN 0-19-506646-2 (paperback), Polym. Int. 25 (1991) 258. https://doi.org/10.1002/pi.4990250415.

[22] A.J. Kinloch (Ed.), Structural adhesives: Developments in resins and primers, Elsevier Applied Science, London, 1986.

[23] Manufacturing processes for advanced composites, Elsevier, New York, 2004.

[24] R.N. Haward, R.J. Young (Eds.), The Physics of Glassy Polymers, Springer Netherlands, Dordrecht, s.l., 1997.

[25] J.-P. Pascault, H. Sautereau, J. Verdu, R.J.J. Williams, Thermosetting Polymers, CRC Press, 2002.

[26] R.J. Day, P.A. Lovell, D. Pierre, Toughening of epoxy resins using particles prepared by emulsion polymerization: effects of particle surface functionality, size and morphology on impact fracture properties, Polym. Int. 44 (1997) 288–299. https://doi.org/10.1002/(SICI)1097-0126(199711)44:3<288:AID-PI866>3.0.CO;2-B.

[27] J.Y. Qian, R.A. Pearson, V.L. Dimonie, M.S. El-Aasser, Synthesis and application of core–shell particles as toughening agents for epoxies, J. Appl. Polym. Sci. 58 (1995) 439–448. https://doi.org/10.1002/app.1995.070580222.

[28] S. Jingqiang, Z. Yafeng, Q. Jindong, K. Jianzheng, Core-shell particles with an acrylate polyurethane core as tougheners for epoxy resins, J Mater Sci 39 (2004) 6383–6384. https://doi.org/10.1023/B:JMSC.0000043763.65417.4f.

[29] R.J. Day, P.A. Lovell, A.A. Wazzan, Toughened carbon/epoxy composites made by using core/shell particles, Composites Science and Technology 61 (2001) 41–56. https://doi.org/10.1016/S0266-3538(00)00169-X.

[30] L. Bcu-Longuet, A. Bonnet, C. Pichot, H. Sautereau, A. Maazouz, Epoxy networks toughened by core-Shell particles: Influence of the particle structure and size on the rheological and mechanical properties, J. Appl. Polym. Sci. 72 (1999) 849–858. https://doi.org/10.1002/(SICI)1097-4628(19990509)72:6<849:AID-APP10>3.0.CO;2-R.

[31] K.-F. Lin, Y.-D. Shieh, Core-shell particles designed for toughening the epoxy resins. II. Core-shell-particle-toughened epoxy resins, J. Appl. Polym. Sci. 70 (1998) 2313–2322. https://doi.org/10.1002/(SICI)1097-4628(19981219)70:12<2313:AID-APP2>3.0.CO;2-P.

[32] R.A. Pearson, A.F. Yee, Influence of particle size and particle size distribution on toughening mechanisms in rubber-modified epoxies, J Mater Sci 26 (1991) 3828–3844. https://doi.org/10.1007/BF01184979.

[33] B.S. Hayes, J.C. Seferis, Modification of thermosetting resins and composites through preformed polymer particles: A review, Polym. Compos. 22 (2001) 451–467. https://doi.org/10.1002/pc.10551.

[34] G. Giannakopoulos, K. Masania, A.C. Taylor, Toughening of epoxy using core–shell particles, J Mater Sci 46 (2011) 327–338. https://doi.org/10.1007/s10853-010-4816-6.

[35] C.K. Riew, A.R. Siebert, R.W. Smith, M. Fernando, A.J. Kinloch, Toughened Epoxy Resins: Preformed Particles as Tougheners for Adhesives and Matrices, in: C.K. Riew (Ed.), Novel approaches in science and engineering: Developed from a symposium … at the 207th national meeting of the American Chemical Society, San Diego, California, American Chemical Society, Washington, DC, 1996, pp. 33–44.

[36] S.-A. Xu, X.-X. Song, Introduction to Rubber Toughened Epoxy Polymers, in: J. Pionteck, E.M. Woo, N. Hameed (Eds.), Handbook of Epoxy Blends, Springer, Cham, 2017, pp. 3–28.

[37] J. Cha, G.H. Jun, J.K. Park, J.C. Kim, H.J. Ryu, S.H. Hong, Improvement of modulus, strength and fracture toughness of CNT/Epoxy nanocomposites through the functionalization of carbon nanotubes, Composites Part B: Engineering 129 (2017) 169–179. https://doi.org/10.1016/j.compositesb.2017.07.070.

[38] W.D. Bascom, R.L. Cottington, Effect of Temperature on the Adhesive Fracture Behavior of an Elastomer-Epoxy Resin, The Journal of Adhesion 7 (1976) 333–346. https://doi.org/10.1080/00218467608075063.

[39] Y. Huang, A.J. Kinloch, Modelling of the toughening mechanisms in rubber-modified epoxy polymers, J Mater Sci 27 (1992) 2763–2769. https://doi.org/10.1007/BF00540703.

[40] P. Cheang, K.A. Khor, Addressing processing problems associated with plasma spraying of hydroxyapatite coatings, Biomaterials 17 (1996) 537–544. https://doi.org/10.1016/0142-9612(96)82729-3.

[41] T.W. Bauer, R.C. Geesink, R. Zimmerman, J.T. McMahon, Hydroxyapatite-coated femoral stems. Histological analysis of components retrieved at autopsy, J. Bone Joint Surg. Am. 73 (1991) 1439–1452.

[42] B. Ribeiro, E.C. Botelho, M.L. Costa, C.F. Bandeira, Carbon nanotube buckypaper reinforced polymer composites: a review, Polímeros 27 (2017) 247–255. https://doi.org/10.1590/0104-1428.03916.

[43] C. Li, Elastic moduli of multi-walled carbon nanotubes and the effect of van der Waals forces, Composites Science and Technology 63 (2003) 1517–1524. https://doi.org/10.1016/S0266-3538(03)00072-1.

[44] E.T. Thostenson, T.-W. Chou, On the elastic properties of carbon nanotube-based composites: modelling and characterization, J. Phys. D: Appl. Phys. 36 (2003) 573–582. https://doi.org/10.1088/0022-3727/36/5/323.

[45] D. Qian, E.C. Dickey, R. Andrews, T. Rantell, Load transfer and deformation mechanisms in carbon nanotube-polystyrene composites, Appl. Phys. Lett. 76 (2000) 2868–2870. https://doi.org/10.1063/1.126500.

[46] F.H. Gojny, M.H.G. Wichmann, U. Köpke, B. Fiedler, K. Schulte, Carbon nanotube-reinforced epoxy-composites: enhanced stiffness and fracture toughness at low nanotube content, Composites Science and Technology 64 (2004) 2363–2371. https://doi.org/10.1016/j.compscitech.2004.04.002.

[47] F.H. Gojny, M.H.G. Wichmann, B. Fiedler, W. Bauhofer, K. Schulte, Influence of nano-modification on the mechanical and electrical properties of conventional fibre-reinforced composites, Composites Part A: Applied Science and Manufacturing 36 (2005) 1525–1535. https://doi.org/10.1016/j.compositesa.2005.02.007.

[48] L.-C. Tang, Y.-J. Wan, K. Peng, Y.-B. Pei, L.-B. Wu, L.-M. Chen, L.-J. Shu, J.-X. Jiang, G.-Q. Lai, Fracture toughness and electrical conductivity of epoxy composites filled with carbon nanotubes and spherical particles, Composites Part A: Applied Science and Manufacturing 45 (2013) 95–101. https://doi.org/10.1016/j.compositesa.2012.09.012.

[49] J. Cha, S. Jin, J.H. Shim, C.S. Park, H.J. Ryu, S.H. Hong, Functionalization of carbon nanotubes for fabrication of CNT/epoxy nanocomposites, Materials & Design 95 (2016) 1–8. https://doi.org/10.1016/j.matdes.2016.01.077.

[50] B. Saboori, M.R. Ayatollahi, Experimental fracture study of MWCNT/epoxy nanocomposites under the combined out-of-plane shear and tensile loading, Polymer Testing 59 (2017) 193–202. https://doi.org/10.1016/j.polymertesting.2017.01.028.

[51] M. Nazem Salimi, M. Torabi Merajin, M.K. Besharati Givi, Enhanced mechanical properties of multifunctional multiscale glass/carbon/epoxy composite reinforced with carbon nanotubes and simultaneous carbon nanotubes/nanoclays, Journal of Composite Materials 51 (2017) 745–758. https://doi.org/10.1177/0021998316655201.

[52] M.R. Ayatollahi, S. Shadlou, M.M. Shokrieh, Fracture toughness of epoxy/multi-walled carbon nanotube nano-composites under bending and shear loading conditions, Materials & Design 32 (2011) 2115–2124. https://doi.org/10.1016/j.matdes.2010.11.034.

[53] H. Xu, X. Tong, Y. Zhang, Q. Li, W. Lu, Mechanical and electrical properties of laminated composites containing continuous carbon nanotube film interleaves, Composites Science and Technology 127 (2016) 113–118. https://doi.org/10.1016/j.compscitech.2016.02.032.

[54] N. Zheng, Y. Huang, H.-Y. Liu, J. Gao, Y.-W. Mai, Improvement of interlaminar fracture toughness in carbon fiber/epoxy composites with carbon nanotubes/polysulfone interleaves, Composites Science and Technology 140 (2017) 8–15. https://doi.org/10.1016/j.compscitech.2016.12.017.

[55] H. Zhou, X. Du, H.-Y. Liu, H. Zhou, Y. Zhang, Y.-W. Mai, Delamination toughening of carbon fiber/epoxy laminates by hierarchical carbon nanotube-short carbon fiber interleaves, Composites Science and Technology 140 (2017) 46–53. https://doi.org/10.1016/j.compscitech.2016.12.018.

[56] D.C. Davis, B.D. Whelan, An experimental study of interlaminar shear fracture toughness of a nanotube reinforced composite, Composites Part B: Engineering 42 (2011) 105–116. https://doi.org/10.1016/j.compositesb.2010.06.001.

[57] X. Du, F. Xu, H.-Y. Liu, Y. Miao, W.-G. Guo, Y.-W. Mai, Improving the electrical conductivity and interface properties of carbon fiber/epoxy composites by low temperature flame growth of carbon nanotubes, RSC Adv. 6 (2016) 48896–48904. https://doi.org/10.1039/C6RA09839H.

[58] Hexion: EpikoteTM Resin 828: Safety Data Sheet, 2022.

[59] H. Petersen, Bisphenol-A-Diglycidylether: Vorkommen, Ersatzstoffe und Reaktionen mit Lebensmittelbestandteilen, 2003.

[60] Hexion: EPIKURE™ Curing Agent MGS RIMH 137: Safety Data Sheet, 2017.

[61] H. Voormann, Smart dispersion of carbon nanoparticle epoxy composites: from nano to application, 2021.

[62] Z. Spitalsky, D. Tasis, K. Papagelis, C. Galiotis, Carbon nanotube–polymer composites: Chemistry, processing, mechanical and electrical properties, Progress in Polymer Science 35 (2010) 357–401. https://doi.org/10.1016/j.progpolymsci.2009.09.003.

[63] J. Li, P.C. Ma, W.S. Chow, C.K. To, B.Z. Tang, J.-K. Kim, Correlations between Percolation Threshold, Dispersion State, and Aspect Ratio of Carbon Nanotubes, Adv. Funct. Mater. 17 (2007) 3207–3215. https://doi.org/10.1002/adfm.200700065.

[64] Schill+Seilacher STRUKTOL POLYCAVIT 3565: Safety Data Sheet, 2020.

[65] Schill+Seilacher STRUKTOL POLYDIS 3614: Safety Data Sheet, 2020.

[66] D20 Committee, Test Methods for Plane-Strain Fracture Toughness and Strain Energy Release Rate of Plastic Materials, ASTM International, West Conshohocken, PA.

[67] J. Ma, M.-S. Mo, X.-S. Du, P. Rosso, K. Friedrich, H.-C. Kuan, Effect of inorganic nanoparticles on mechanical property, fracture toughness and toughening mechanism of two epoxy systems, Polymer 49 (2008) 3510–3523. https://doi.org/10.1016/j.polymer.2008.05.043.

[68] Y.L. Liang, R.A. Pearson, Toughening mechanisms in epoxy–silica nanocomposites (ESNs), Polymer 50 (2009) 4895–4905. https://doi.org/10.1016/j.polymer.2009.08.014.

[69] B.B. Johnsen, A.J. Kinloch, R.D. Mohammed, A.C. Taylor, S. Sprenger, Toughening mechanisms of nanoparticle-modified epoxy polymers, Polymer 48 (2007) 530–541. https://doi.org/10.1016/j.polymer.2006.11.038.

[70] L. Becu, A. Maazouz, H. Sautereau, J.F. Gerard, Fracture behavior of epoxy polymers modified with core-shell rubber particles, J. Appl. Polym. Sci. 65 (1997) 2419–2431. https://doi.org/10.1002/(SICI)1097-4628(19970919)65:12<2419:AID-APP14>3.0.CO;2-W.

[71] S. Saseendran, M. Wysocki, J. Varna, Cure-state dependent viscoelastic Poisson's ratio of LY5052 epoxy resin, Advanced Manufacturing: Polymer & Composites Science 3 (2017) 92–100. https://doi.org/10.1080/20550340.2017.1348002.

[72] Š. Dvořáčková, D. Kroisová, Thermal Expansion of Composite System Epoxy Resin/Recycled Carbon Fibers, MSF 994 (2020) 162–169. https://doi.org/10.4028/www.scientific.net/MSF.994.162.

[73] L. Deng, R.J. Young, I.A. Kinloch, R. Sun, G. Zhang, L. Noé, M. Monthioux, Coefficient of thermal expansion of carbon nanotubes measured by Raman spectroscopy, Appl. Phys. Lett. 104 (2014) 51907. https://doi.org/10.1063/1.4864056.

[74] T.H. Hsieh, A.J. Kinloch, K. Masania, J. Sohn Lee, A.C. Taylor, S. Sprenger, The toughness of epoxy polymers and fibre composites modified with rubber microparticles and silica nanoparticles, J Mater Sci 45 (2010) 1193–1210. https://doi.org/10.1007/s10853-009-4064-9.

[75] A.J. Kinloch, A.C. Taylor, The toughening of cyanate-ester polymers Part I Physical modification using particles, fibres and woven-mats, J Mater Sci 37 (2002) 433–460. https://doi.org/10.1023/A:1013735103120.

[76] Y. Huang, A.J. Kinloch, The role of plastic void growth in the fracture of rubber-toughened epoxy polymers, J Mater Sci Lett 11 (1992) 484–487. https://doi.org/10.1007/BF00731112.

[77] A.F. Yee, D. Li, X. Li, The importance of constraint relief caused by rubber cavitation in the toughening of epoxy, J Mater Sci 28 (1993) 6392–6398. https://doi.org/10.1007/BF01352202.

[78] R.A. Pearson, A.F. Yee, Toughening mechanisms in elastomer-modified epoxies, J Mater Sci 24 (1989) 2571–2580. https://doi.org/10.1007/BF01174528.

[79] A.J. Kinloch, S.J. Shaw, D.A. Tod, D.L. Hunston, Deformation and fracture behaviour of a rubber-toughened epoxy: 1. Microstructure and fracture studies, Polymer 24 (1983) 1341–1354. https://doi.org/10.1016/0032-3861(83)90070-8.

[80] A.N. Gent, Fracture in polymers. E. H. Andrews, American Elsevier, New York, 1968, J. Polym. Sci. A-2 Polym. Phys. 7 (1969) 747. https://doi.org/10.1002/pol.1969.160070413.